Science of the Total Environment 779 (2021) 146501

Contents lists available at ScienceDirect

Science of the Total Environment

journal homepage: www.elsevier.com/locate/scitotenv

Fermentation, methanotrophy and methanogenesis influence sedimentary Fe and As dynamics in As-affected aquifers in Vietnam

Martyna Glodowska [a,b,c,*], Magnus Schneider [d], Elisabeth Eiche [d], Agnes Kontny [d], Thomas Neumann [e], Daniel Straub [b,f], Michael Berg [g], Henning Prommer [h,i], Benjamin C. Bostick [j], Athena A. Nghiem [j], Sara Kleindienst [b], Andreas Kappler [a]

[a] Geomicrobiology, Center for Applied Geosciences, University of Tübingen, Germany
[b] Microbial Ecology, Center for Applied Geosciences, University of Tübingen, Germany
[c] Department of Microbiology, IWWR, Radboud University, the Netherlands
[d] Karlsruhe Institute of Technology, Institute of Applied Geosciences, Germany
[e] Technical University of Berlin, Institute for Applied Geosciences, Berlin, Germany
[f] Quantitative Biology Center (QBiC), University of Tübingen, Germany
[g] Eawag, Swiss Federal Institute of Aquatic Science and Technology, Dübendorf, Switzerland
[h] School of Earth Sciences, University of Western Australia, Perth, WA, Australia
[i] CSIRO Land and Water, Floreat, WA, Australia
[j] Lamont-Doherty Earth Observatory, Columbia University, USA

HIGHLIGHTS

- Fermentation, methanogenesis and methanotrophy prevail at the As-contaminated site.
- Reducing aquifer consists of gray sediment and is dominated by Fe(III) (oxyhydr)oxides and As(III).
- Less reducing aquifer consists of yellow-brown sediment and is dominated by goethite and As(V).
- Anaerobic CH_4 oxidation likely supports carbonate mineral formation.
- Methanotrophic Fe(III)-reducer Ca. Methanoperedens coincides with As and Fe peaks in sediments.

GRAPHICAL ABSTRACT

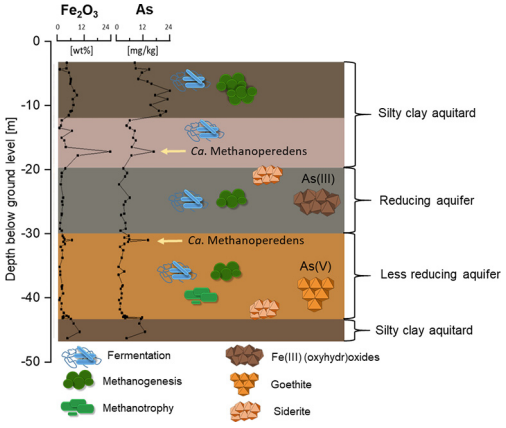

ARTICLE INFO

Article history:
Received 19 January 2021
Received in revised form 24 February 2021
Accepted 11 March 2021
Available online 17 March 2021

Editor: Jurgen Mahlknecht

ABSTRACT

High arsenic (As) concentrations in groundwater are a worldwide problem threatening the health of millions of people. Microbial processes are central in the (trans)formation of the As-bearing ferric and ferrous minerals, and thus regulate dissolved As levels in many aquifers. Mineralogy, microbiology and dissolved As levels can vary sharply within aquifers, making high-resolution measurements particularly valuable in understanding the linkages between them. We conducted a high spatial resolution geomicrobiological study in combination with analysis of sediment chemistry and mineralogy in an alluvial aquifer system affected by geogenic As in the Red River delta in Vietnam. Microbial community analysis revealed a dominance of fermenters, methanogens and methanotrophs whereas sediment mineralogy along a 46 m deep core showed a diversity of Fe minerals

* Corresponding authora at: Department of Microbiology, IWWR, Radboud University, The Netherlands.
E-mail address: m.glodowska@science.ru.nl (M. Glodowska).

https://doi.org/10.1016/j.scitotenv.2021.146501

Keywords:
Iron minerals
Methane formation
Methane oxidation
Arsenic
Groundwater system

including poorly crystalline Fe (II/III) and Fe(III) (oxyhydr)oxides such as goethite, hematite, and magnetite, but also the presence of Fe(II)-bearing carbonates and sulfides which likely formed as a result of microbially driven organic carbon (OC) degradation. A potential important role of methane (CH_4) as electron donor for reductive Fe mineral (trans)formation was supported by the high abundance of *Candidatus* Methanoperedens, a known Fe(III)-reducing methanotroph. Overall, these results imply that OC turnover including fermentation, methanogenesis and CH_4 oxidation are important mechanisms leading to Fe mineral (trans)formation, dissolution and precipitation, and thus indirectly affecting As mobility by changing the Fe-mineral inventory.

1. Introduction

Exposure to arsenic (As) is considered a major public health concern due to its toxic effects on human health (Muehe and Kappler, 2014; Water et al., 1999). The International Agency for Research on Cancer (IARC) defines As as a group I human carcinogen and the U.S. Agency for Toxic Substances and Disease Registry (ATSDR) placed it at the highest position on the priority list (Naujokas et al., 2013). Geogenic As in drinking water from groundwater resources is the major source of As to most people (WHO). In many areas, As is fairly prevalent in shallow groundwater (Smedley and Kinniburgh, 2002). Up to 220 million people are potentially exposed to As concentrations in groundwater above the WHO limit of 10 μg/L, with the majority of exceedances (94%) occurring in Asia (Podgorski and Berg, 2020). This is particularly concerning since many communities from developing countries of South and Southeast Asia lack access to water treatment facilities and thus, still largely depend on untreated groundwater from shallow wells.

It is widely accepted that As in shallow groundwater bodies in South and Southeast Asia is mainly of geogenic origin. Arsenic-loaded sediments washed down the slopes of the Himalayan Mountains were transported in the past and still continue being deposited in floodplains of the Red River, Mekong, Ganges and Indus Deltas as well as in West Bengal. Subsequent release of As from these young sediments to groundwater occurs through several mechanisms.

Most As mobilization is attributed the microbially mediated reductive dissolution of As-bearing Fe(III) (oxyhydr)oxide minerals (Chatain et al., 2005; Harvey et al., 2002; Islam et al., 2004; Neumann et al., 2014; Zhu et al., 2017), a process that is coupled to the oxidation of organic carbon (OC) co-deposited with As-bearing sediment. Oxidation of As-rich sulfides (mainly pyrites), competitive sorption and exchange of As with phosphate (PO_4^{3-}) or changes in sorption capacities of As-bearing Fe(III) (oxyhydr)oxides also can be important in some environments (Chowdhury et al., 1999; Smedley and Kinniburgh, 2002). These processes, however, can be relevant only under specific conditions, e.g., when As-rich iron sulfides are abundant in sediments or when high PO_4^{3-} input to the aquifer occurs.

Microorganisms can affect the fate of As in aquifers in many different ways, but most importantly through their role in Fe mineral (trans)formation, given that poorly crystalline Fe(III) (oxyhydr)oxides such as ferrihydrite (Fh), are important As-hosting phases in As-contaminated aquifers (Ravenscroft et al., 2011). Ferrihydrite or nanoparticulate Fe (oxyhydr)oxides form via abiotic or microbial Fe(II) oxidation (Cornell and Schwertmann, 2003), and are preferentially used as a terminal electron acceptor by Fe(III)-reducing microorganisms (Lovley et al., 1991). Moreover, Fh is a precursor of more crystalline Fe(III) oxides like goethite or hematite (Zachara et al., 2002).

Various microorganisms such as *Geobacter* spp.(Islam et al., 2005a, 2005b), *Shewanella* spp.(Cummings et al., 1999) and *Geothrix* spp. (Islam et al., 2005a) were found to be capable of reducing Fe(III) minerals while oxidizing sedimentary or dissolved organic matter (OM). In addition, several recent studies demonstrated that anaerobic CH_4-oxidizing archaea are also able to use Fe(III) as electron acceptor (Aromokeye et al., 2020; Cai et al., 2018; Egger et al., 2015; Ettwig et al., 2016). The prevalence and specific role of CH_4 as a carbon donor for Fe(III) reduction, however, requires further study.

Microbially mediated anaerobic oxidation of CH_4 is often associated with a clear mineralogical signature of carbonate precipitation (Reitner et al., 2005). This occurs through two steps. First, anaerobic oxidation of CH_4, either coupled to SO_4^{2-}, NO_3^-, NO_2^-, Fe(III) or Mn(IV) reduction, can increase water bicarbonate alkalinity according to:

$$CH_4 + {SO_4}^{2-} \rightarrow {HCO_3}^- + HS^- + H_2O \quad (1)$$

$$5CH_4 + 8{NO_3}^- + 3H^+ \rightarrow 5{HCO_3}^- + 4\,N_2 + 9H_2O \quad (2)$$

$$3CH_4 + 8{NO_2}^- + 5H^+ \rightarrow 3{HCO_3}^- + 8\,N_2 + 7H_2O \quad (3)$$

$$CH_4 + 8Fe(OH)_3 + 15H^+ \rightarrow {HCO_3}^- + 8Fe^{2+} + 21H_2O \quad (4)$$

$$CH_4 + 4MnO_2 + 7H^+ \rightarrow {HCO_3}^- + 4Mn^{2+} + H_2O \quad (5)$$

The second step, i.e., the increase in bicarbonate alkalinity, often triggers the precipitation of carbonate minerals as the joint release of cations like Fe^{2+} and Mn^{2+} produced by anaerobic microbial oxidation of CH_4 leads to carbonate mineral supersaturation (Aloisi et al., 2002). In reduced sediments, authigenic carbonate formation can be promoted by the presence of additional bicarbonate or carbon dioxide (CO_2) produced during anaerobic decomposition of organic matter (Lein et al., 2002). In the case of Fe(III) reduction (reaction (4)) the precipitation may consume the majority of the Fe^{2+} that is produced or other cations from the aquifer, e.g.:

$$Fe^{2+} + {HCO_3}^- \rightarrow FeCO_3 + H^+ \quad (6)$$

The overall process (reactions (4) + (6)), thus is slightly less pH dependent, and produces extensive carbonate minerals. We thus expect extensive Fe carbonates in zones where anaerobic oxidation of CH_4 is prevalent.

Some previous studies indicated that $CaCO_3$ might play a role in As immobilization via $CO_3^{2-} \leftrightarrow AsO_3^{3-}$ substitution (Bardelli et al., 2011). It was also shown that As(V), which is the thermodynamically favored species under oxic conditions, strongly adsorbs on calcite surfaces, thereby significantly decreasing its mobility (Sø et al., 2008). However, As(III), which is typically the dominating species under reducing conditions, does not sorb on calcite. It has therefore been concluded that sorption of As on calcite is of little relevance under reducing conditions where As(III) is the dominating species (Yokoyama et al., 2012). Competitive displacement of As by carbonate on Fe(III) (oxyhydr)oxides, was also proposed as a potential mechanism of As mobilization from Fe-rich sediments (Appelo et al., 2002). However, it was shown that although carbonate anions do compete with As for adsorption to Fe(III) (oxyhydr)oxide-coated sand, the competitive effect was relatively small with regard to the total concentration of adsorbed As and relative to the potentially much more pronounced competitive effects of PO_4^{3-} (Radu et al., 2005).

In many As-contaminated subsurface environments, including reducing aquifers across South and Southeast Asia, both dissolved carbonate and dissolved Fe^{2+} are commonly present at relatively high concentrations. These conditions favor the formation of Fe carbonate complexes (King, 1998) and the precipitation of Fe carbonate minerals ($FeCO_3$).

Although, some studies suggested that $FeCO_3$ (siderite) might sorb significant amounts of As(III) and As(V) (Guo et al., 2007), this is mainly the case for As(V) (Guo et al., 2010; Jönsson and Sherman, 2008). Yet, As (III) accounts for the majority of dissolved As under reducing condition, therefore this process is likely less relevant. It is therefore evident that the role of carbonate minerals that are ubiquitous in areas where anaerobic CH_4 oxidation occurs, needs to be critically evaluated in order to better understand As cycling under these conditions.

Sulfur cycling, and in particular sulfate reduction, often also plays an important role in As mobility. Sulfide (S^{2-}) produced via microbially mediated sulfate (SO_4^{2-}) reduction under strongly reducing conditions, can precipitate Fe and thereby co-precipitate As. Various Fe(II) sulfides such as pyrite, mackinawite and troilite show a remarkable sorption affinity towards As (Bostick et al., 2004; Bostick and Fendorf, 2003; Kirk et al., 2004; Lowers et al., 2007). Additionally, As can also form pure phases (e.g., realgar (AsS), orpiment (As_2S_3)) or metal-As sulfides (e.g., arsenopyrite (FeAsS)) (Newman et al., 1997). Although Fe(II) sulfides are usually less abundant in delta aquifer sediments compared to Fe(III) (oxyhydr)oxides due to a limited supply of sulfur in freshwater environments, SO_4^{2-} reduction is generally linked to a decrease of As concentrations in water (Buschmann & Berg, 2009; Kirk et al., 2004; Rittle et al., 1995) and precipitation of As with Fe sulfides has been proposed as remediation strategy for As contaminated groundwater (Keimowitz et al., 2007; Omoregie et al., 2013; Pi et al., 2017). Various adsorbed, coprecipitated and specific mineral phases in reducing sediments, however, are seldom investigated in relation to microbial processes.

Therefore, the objectives of this study were to investigate the microbial communities and their involvement in biogeochemical cycles of CH_4, Fe, As, and to lower extent S. We aimed to identify the relevant microbial processes in the aquifer sediments and their potential direct or indirect impact on Fe mineralogy and As mobility. Our study highlights the importance of CH_4 which can be a relevant intermediate in microbially mediated Fe mineral (trans)formation at the redox transition zone (RTZ).

2. Materials and methods

2.1. Study area and sample collection

Van Phuc is a village located within a meander of the Red River (20°55′18.8″N, 105°53′38.3″E) about 15 km Southeast from Hanoi, Vietnam. The groundwater below Van Phuc is characterized by varying As concentrations that locally exceed 500 μg/L in the strongly reducing Holocene sections of the aquifer, while generally remaining below 10 μg/L in the less reducing Pleistocene sections of the aquifer. The transition between these two aquifers is characterized by sharply changing redox conditions (Fig. 1). Detailed descriptions of the study site, including its key geological, mineralogical, lithologic and hydrochemical characteristics were provided previously (Eiche et al., 2008, 2017; Nghiem et al., 2020; Stopelli et al., 2020). An interesting feature of this site is a nearly flammable concentration of CH_4 (over 50 mg/L) in some of the groundwater wells (Glodowska et al., 2020c). Similarly to many other As-contaminated sites, the CH_4 concentration in Van Phuc is positively correlated with high dissolved Fe and As concentrations (Stopelli et al., 2020).

Sediment samples from Van Phuc were taken by rotary drilling at the redox transition zone (RTZ), which divides the As-contaminated (high As concentration in groundwater) from the uncontaminated part of the aquifer (low As concentration in groundwater). At its top, the aquifer is overlain with a silty clay aquitard of ~20 m thickness, which is organic-rich in some layers (Figs. 1 and 2). In the upper part of the aquifer (at 20–30 m depth below ground), the groundwater is most reducing and has the highest As (up to 400 μg/L), Fe (13 mg/L) and CH_4 concentrations (up to 51 mg/L) (Glodowska et al., 2020c). This part consists predominantly of gray sediments, thus implying that at least a partial reduction of Fe(III) minerals occurred. On the contrary, groundwater in the lower part of the RTZ (30–42.5 m) is characterized by As concentration below 10 μg/L, trace concentration of Fe and no CH_4. Sediments in the lower part of the RTZ are predominantly yellow to brown, indicating that reduction of these Fe(III) minerals has not occurred at this depth. Below 42.5 m depth, an underlying aquitard consisting of silty clay but poorer in total C compared to the upper aquitard has a thickness of nearly 4 m. It is underlain by a gravel layer at 46 m depth (Fig. 1).

In October 2018, sediment cores (10 cm in diameter; each individual piece ca. 3 m long) were collected using a rotary drilling technique to a depth of up to 46 m below ground level. Core characterization for sediment lithology, color, grain size, magnetic susceptibility and a photographic documentation was performed in the field directly after core segments were opened. Each sediment core was halved using a ceramic knife. After core characterization, subsamples were collected from the central part of the core to minimize contamination with drilling fluids. For microbial community analysis, sediments were collected with ethanol sterilized spatula into sterile 15 mL Falcon tubes. Collected sediments were immediately immersed in LifeGuard Soil Preservation Solution (Qiagen) in order to stabilize the microbial DNA and RNA. Samples were stored on dry ice during transport and placed in a −80 °C freezer upon arrival at the laboratory until analysis. For the geochemical and mineralogical analysis, bulk sediments flushed with N_2 in the field were collected (n = 69). All samples were cooled immediately after

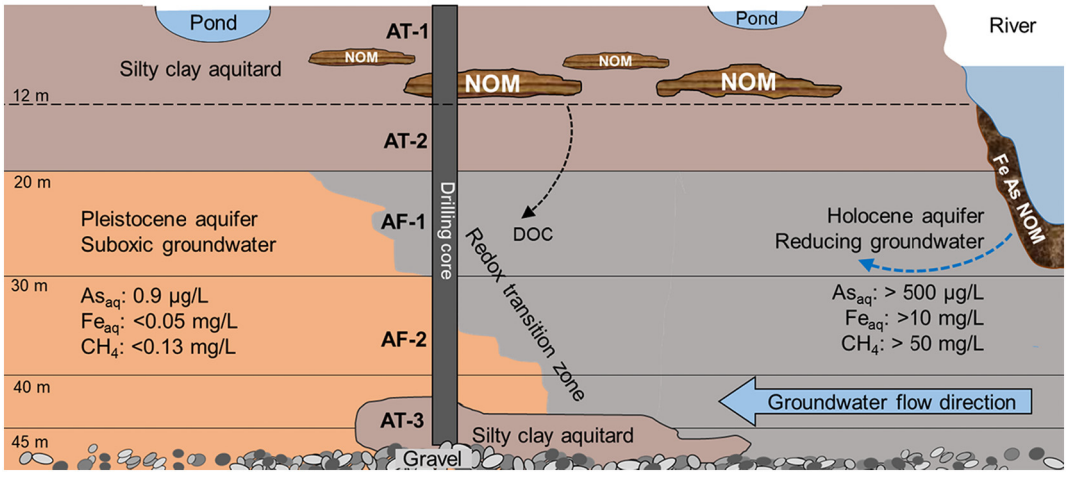

Fig. 1. Two-dimensional cross-section of Van Phuc aquifer with the redox transition zone (RTZ) which divides gray As-contaminated aquifer of Holocene origin (AF-1) and Pleistocene non-contaminated aquifer consisting of yellow-brown sediments (AF-2).

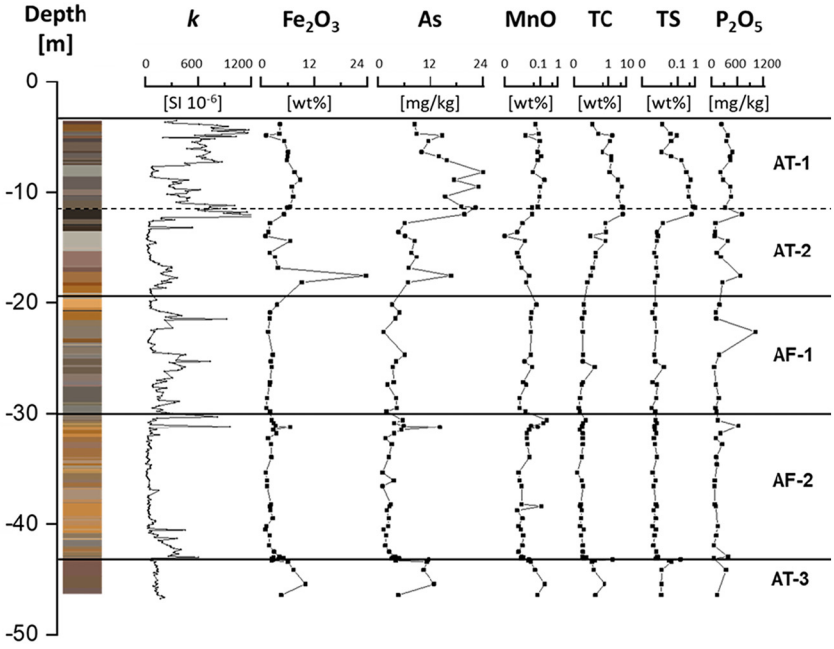

Fig. 2. Vertical profiles of the redox transition zone including changes in magnetic susceptibility (k) as well as Fe, As, Mn, total carbon (TC), total sulfur (TS) and P. Note that MnO, TC and TS have a logarithmic scale for better visibility, and k is cut off at 1200×10^{-6} SI for scale issues. The sediment profile consists of top aquitard (AT-1 and AT-2), gray Holocene aquifer (AF-1), yellow-brown Pleistocene aquifer (AF-2) and bottom aquitard (AT-3).

sampling and during transport to minimize microbial activity and alteration of the Fe mineralogy. Water- and air-tight pouches with zip (PET/PE-LD/Aluminium stand-up pouches LamiZip, (DAKLAPACK)) preventing oxygen, vapour and UV radiation were used to minimize sample alteration.

2.2. Microbial community analysis

2.2.1. DNA extraction, 16S rRNA gene sequence analysis and quantitative PCR

DNA was extracted using a phenol-chloroform method following a protocol from Lueders et al. (2004). DNA was eluted in 50 μL of a 10 mM Tris buffer. DNA concentrations were determined using a Qubit® 2.0 Fluorometer with DNA HS kits (Life Technologies, Carlsbad, CA, USA). Bacterial and archaeal 16S rRNA genes were amplified using universal primers 515f: GTGYCAGCMGCCGCGGTAA (Parada et al., 2016) and 806r: GGACTACNVGGGTWTCTAAT (Apprill et al., 2015) fused to Illumina adapters. The PCR cycling conditions were as follows: 95 °C for 3 min, 25 cycles of 95 °C for 30 s, 55 °C for 30 s, and 75 °C for 30 s. This was followed by a final elongation step at 72 °C for 3 min. The quality and quantity of the purified amplicons were determined using agarose gel electrophoresis and NanoDrop (NanoDrop 1000, Thermo Scientific, Waltham, MA, USA). Subsequent library preparation steps and Illumina MiSeq sequencing (Illumina, San Diego, CA, USA) using the 2 × 250 bp MiSeq Reagent Kit v2 (500 cycles kit) were performed at Microsynth AG (Balgach, Switzerland). Between 38,425 and 172,443 read pairs were obtained for each sample.

Sequencing data was analyzed with nf-core/ampliseq v1.0.0, which includes all analysis steps and software and is publicly available (Ewels et al., 2020; Straub et al., 2019). Primers were trimmed, and untrimmed sequences were discarded (<10% per sample) with Cutadapt version 1.16 (Martin, 2011). Adapter and primer-free sequences were imported into QIIME2 version 2018.06 (Bolyen et al., 2018), their quality was checked with demux (https://github.com/qiime2/q2-demux), and they were processed with DADA2 version 1.6.0 (Callahan et al., 2016) to eliminate PhiX contamination, trim reads (before median quality drops below 35; forward reads were trimmed at 230 bp and reverse reads at 200 bp), correct errors, merge read pairs, and remove PCR chimeras; ultimately, 18,510 amplicon sequencing variants (ASVs) were obtained across all samples. Alpha rarefaction curves were produced with the QIIME2 diversity alpha-rarefaction plugin, which indicated that the richness of the samples had been fully observed. A Naive Bayes classifier was fitted with 16S rRNA (gene) sequences extracted from the SILVA version 132 SSU Ref NR 99 database (Pruesse et al., 2007), using the PCR primer sequences. ASVs were classified by taxon using the fitted classifier (https://github.com/qiime2/q2-feature-classifier). ASVs classified as chloroplasts or mitochondria were removed. The number of removed ASVs was 60, totaling to <2% relative abundance per sample, and the remaining ASVs had their abundances extracted by feature table (Pruesse et al., 2007). The abundance table was rarefied with a sampling depth of 26,162 - the number of minimum counts across samples - and Bray-Curtis dissimilarities were calculated with q2-diversity (https://github.com/qiime2/q2-diversity).

Pathways, i.e. MetaCyc ontology predictions, were inferred with PICRUSt2 version 2.2.0-b (Phylogenetic Investigation of Communities by Reconstruction of Unobserved States) (Langille et al., 2013) and MinPath (Minimal set of Pathways) (Ye and Doak, 2009) using ASVs and their abundance counts. Inferring metabolic pathways from 16S rRNA amplicon sequencing data is not as accurate as measuring genes by shotgun metagenomics, but it yields helpful approximations to support hypotheses driven by additional microbiological and biogeochemical analyses (Langille et al., 2013).

Raw sequencing data have been deposited at GenBank under BioProject accession number PRJNA669416 (https://www.ncbi.nlm.nih.gov/bioproject/PRJNA669416) and the sample at 39.7 m depth was previously deposited as SRR10590531, BioSample SAMN13483907 in BioProject PRJNA593718.

Quantitative PCRs specific for 16S rRNA genes of bacteria and archaea, methyl-coenzyme M reductase subunit alpha (*mcrA*) genes, particulate methane monooxygenase (*pmoA*) genes, anaerobic arsenite oxidase (*arxA*) genes were performed. The qPCR primer sequences, gene-specific plasmid standards, and details on the thermal programs are given in Table S1. Quantitative PCRs on DNA extracts obtained as described above were performed in triplicate using SybrGreen® Supermix (Bio-Rad Laboratories GmbH, Munich, Germany) on the C1000 Touch

thermal cycler (CFX96™ real time system). Each quantitative PCR assay was repeated three times, with triplicate measurements calculated for each sample per run. Data analysis was done using the Bio-Rad CFX Maestro 1.1 software version 4.1 (Bio-Rad, 2017).

2.3. Geochemical and mineralogical analysis

Total bulk concentrations (n = 69) of selected major elements given as oxide (K_2O, CaO, MnO, Fe_2O_3), and As were quantified in homogenized sediment material using energy dispersive X-ray fluorescence analysis (XRF) (Epsilon5, PANalytical) with approximately 1 mg/kg detection limit for As. Total carbon (TC) and total sulfur (TS) contents were determined with a carbon-sulfur analyzer (CSA CS-2000, ELTRA). Volume magnetic susceptibility was measured with a handheld SM-30 Kappameter (ZH Instruments) in 10 cm intervals (n = 374) along the halved cores directly in the field.

Iron and As X-ray absorption spectroscopy (XAS) was performed on glycerol-preserved sediment samples at Stanford Synchrotron Radiation Lightsource (SSRL) on beamline 4-1. Eighteen samples were analyzed for Fe, while 22 were analyzed for As. For these measurements, 2 to 3 g of fresh sediment material was taken from the core directly in the field. Blotting paper was used to quickly remove entrained water. Samples were then saturated with an equal volume of glycerol (bidistilled 99.5%, VWR Chemicals) in centrifugation tubes, sealed with parafilm and stored under nitrogen atmosphere to avoid oxidation. The samples were cooled during subsequent storage and transport to 8–12 °C. These samples were then stored in anaerobic bags and frozen (−20 °C) until measurement. Just before measurement, samples were transferred from storage and prepared as thin films sealed in Kapton tape. Each measurement used a Si (220) monochromator, configured with a phi-angle of 90°. Iron K-edge extended X-ray absorption fine structure (EXAFS) was measured with a 32-element Ge detector or passivated implanted planar silicon (PIPS) detector using Soller slits and a 3μx Mn filter as previously described (Nghiem et al., 2020). Iron EXAFS spectra were calibrated with Fe foil (7112.0 eV for the edge inflection point); typically, Soller slits with Mn filter were used with the beam signal detuned to 50%. Arsenic X ray absorption near edge structure (XANES) spectra were collected with the Ge detector using Soller slits and a Ge filter, using spectra calibrated with the Au L edge (11,919 eV). All samples were collected in fluorescence mode with a calibration foil present, with the Fe foil for Fe EXAFS and an Au foil for As XANES in series to permit sample calibration on each scan if needed.

Averaging, background subtraction and normalization of samples spectra for Fe EXAFS was done in SIXPACK; chi files were saved with k-range from 1 to 12. The fraction of different mineral components of Fe were determined from processed spectra using linear combination fitting (LCF) using ferrihydrite, goethite, hematite, green rust sulfate, magnetite, Fe(II/III) silicate (modeled with hornblende), biotite, pyrite and mackinawite, typically with fractional errors of about 0.08–0.1. Following fitting, the fits were normalized to 1 for comparison. These minerals represent mineral groups in some cases rather than specific minerals, in part because structures are often too similar to differentiate minerals based on EXAFS alone. Key to this work, fits may not differentiate ferrihydrite from nanogoethite (Sun et al., 2018). Fe within many silicates also represents a challenge in that there are many Fe-bearing silicates, including many clays, amphiboles and other minerals, many of which contain both Fe(II) and Fe (III). Our fits effectively combine those minerals with a single amphibole, hornblende. The mineral standard green rust sulfate is used to represent green rust, but other green rusts and layered double hydroxides also have similar structures that are difficult to distinguish in mixtures. The fraction of Fe(II) was calculated as fraction of Fe(II) over total Fe using the fraction of each mineral present based on Fe (II) content; hornblende is a variable oxidation state mineral but the reference material we used contains 65% Fe(II) based on previous measurements (Nghiem et al., 2020).

3. Results and discussion

3.1. Sediment geochemistry and mineralogy

3.1.1. Top aquitard section (AT-1 and AT-2)

The sediment geochemistry varies greatly between the different lithologies and is clearly related to sediment color (Fig. 2). In the upper aquitard, down to a depth of approximately 18 m, average concentrations of TC (1.85 ± 2.30 wt%), TS (0.20 ± 0.29 wt%), Fe_2O_3 (5.8 ± 4.6 wt%) and As (13 ± 6 mg/kg) are highest but with a considerable standard deviation, reflecting the geochemical heterogeneity. The aquitard can be clearly separated into two distinct sections (Fig. 2), i.e., an upper section of 12 m thickness (AT-1) and a lower section (AT-2). The upper section contains two times higher As, more than 10 times higher TC and 40 times higher TS concentrations. Earlier studies showed that most of the TC is present as organic carbon throughout the sediment profile (Kontny et al., 2021). The differentiation is also evident from the differences in magnetic susceptibility, which indicates variations in the Fe mineralogy despite a similar Fe_2O_3 content in these two sections of the aquitard. At 17.1 m, directly at the transition of gray and brown sediments and close to the aquitard-aquifer interface, Fe_2O_3 and As concentrations were the highest within the entire sediment profile with 23.7 wt% and 17 mg/kg, respectively.

3.1.2. Highly reduced aquifer section consisting of gray sand (AF-1)

The aquifer can be separated into an upper, mainly gray section (AF-1; 19.7–30.1 m) and a lower, mainly yellow-brown section (AF-2; 30.3–42 m). Interestingly, despite the differences in sediment color, the geochemical composition (TC, TS, MnO, Fe_2O_3, As) is relatively similar for both sections. Peaking Fe_2O_3 (6.5 wt%) and As concentrations (14 mg/kg) occur at the transition between gray and yellow-brown sands (30.7 m). Elevated TC (1.7 wt%), TS (0.15 wt%) and As (12 mg/kg) occur at the lower aquitard-aquifer interface (IF-2; 42.7 m).

There are clear differences regarding magnetic susceptibility, Fe mineralogy and As speciation between the two aquifer sections (Figs. 2 and 3). In general, the gray upper aquifer (AF-1) section has little goethite (mainly <10% of total Fe). The corresponding groundwater in this section of the aquifer is highly reducing with high concentrations of dissolved Fe, As and CH_4 (Glodowska et al., 2020c; Stopelli et al., 2020). This could explain the low proportion of goethite, which is likely dissolved in response to intrusion of reducing water. Although ferrihydrite content is highly variable and often low, at some depths it represents more than 30% of total Fe in the gray aquifer sediments. The presence of ferrihydrite in anoxic sediments suggests that ferrihydrite is either also being produced through anaerobic Fe cycling, or is stabilized (Sun et al., 2021). The reduced portion of the aquifer (AF-1) also contains more elevated fractions of reduced Fe minerals, including Fe sulfides, green rust and magnetite. These minerals are much more abundant in some AF-1 sections of the gray part compared to the AF-2 lower aquifer, which is in agreement with the higher magnetic susceptibility (Figs. 2 and 3). Horneman et al. (2004) previously described that As release is predominantly coupled to the transformation of Fe(III) (oxyhydr)oxide coatings to Fe(II) or mixed Fe(II/III) phases. Moreover, Nghiem et al. (2020) by statistically grouping sediments from aquifer in As affected areas found that gray sediments are generally lower in reactive ferrihydrite but enriched in secondary Fe(II) minerals such as siderite and sulfides which overlaps with our observations. The relatively high content of Fe(III) minerals, especially ferrihydrite, in the gray part of the aquifer (AF-1) could also be related to the reprecipitation of Fe (III) minerals in a coupled process with Mn(IV) reduction as indicated by high resolution investigations in a core that was taken at the same location (Kontny et al., 2021). This is further supported by high concentration of dissolved Mn in the groundwater (Stopelli et al., 2020).

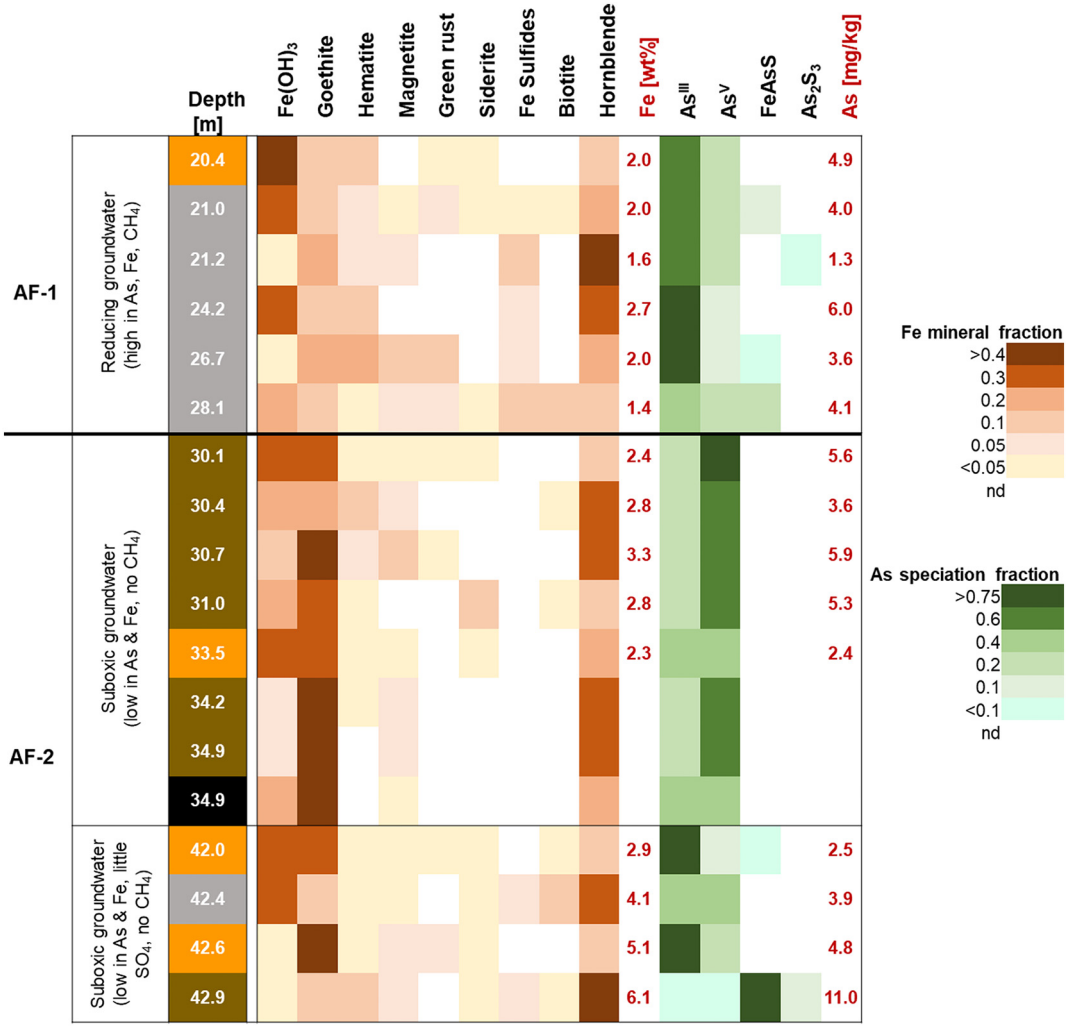

Fig. 3. Heat map showing the relative abundance of Fe minerals and As species in the sediments across the gray Holocene aquifer (AF-1) and yellow-brown Pleistocene aquifer (AF-2) with Fe content given in wt% and As in mg/kg. Fe mineral fraction based on Fe Extended X-ray Absorption Fine Structure (EXAFS) analysis was calculated based on the total Fe content in the given sample. The As species was determined based on X-ray absorption near edge structure (XANES).

Despite the high groundwater CH_4 content and alkalinity in the highly reducing section of the aquifer (AF-1; 20–30 m), Fe carbonates are only present at the upper aquitard-aquifer interface (IF-1; 19.7 m) and at the transition from gray to yellow-brown colored sediments (28.1 m). The absence of siderite could be explained by diverse interactions of carbonate ions with Fe^{2+} and Fe minerals. Chen et al. (2020) showed that goethite tends to aggregate to larger particles in the presence of Fe^{2+} and high alkalinity, which could explain the elevated goethite content in the reduced AF-1 aquifer at 22.2 and 26.7 m (Fig. 3). It is also conceivable that carbonate minerals are not detectable in bulk samples due to their relatively low abundance and their mixed nature (Fe-Mn-Ca carbonates) (Kontny et al., 2021). In the upper part of the aquifer at 20.4 m depth (AF-1), the low proportion of goethite, the presence of green rust, siderite and the dominance of As(III) indicate reducing conditions despite the clearly orange sediment color. We assume that sediment color shows a delayed response to the intrusion of reducing water particularly because it takes many pore volumes in order to change the sediment redox state. Consequently, sediment color alone may not be sufficient to define the redox state of the sediment.

As(III) is mainly dominating (61–85%) in the gray part of the aquifer (AF-1) supporting the predominance of reducing processes in this part (Fig. 3). The proportion of As(III) is gradually decreasing from 27 m towards the transition to yellow brown sand. Furthermore, sulfate reduction appears to play a role in the gray part as indicated by the presence of As bearing sulfides in addition to Fe bearing sulfides. At 28.1 m, FeAsS has a contribution of approximately 30% to the total As speciation. At this depths, also secondary formed Fe(II) minerals such as green rust, siderite, Fe sulfides and magnetite have a relatively high abundance (Fig. 3). The slightly higher As content in many of the gray aquifer samples compared to the less reduced lower aquifer section (AF-2) indicates that Fe minerals precipitation or transformation in this part could be an important sink for dissolved As that is transported from upstream (Fig. 1).

3.1.3. Less reduced aquifer consisting of yellow-brown sand (AF-2)

In the less reduced, yellow-brown aquifer (AF-2; approximately 30–40 m), goethite is the clearly dominating Fe(III) mineral while the abundance of hematite is much lower (<5%) and the content of ferrihydrite is highly variable (Fig. 3). The higher proportion of goethite is expected due to the suboxic nature of the groundwater (little dissolved Fe, As, no SO_4^{2-} and CH_4) at this depth (Glodowska et al., 2020c; Stopelli et al., 2020). This also explains why reduced Fe minerals like Fe sulfides or green rust are generally absent. The dominance of Fe(III) (oxyhydr) oxide minerals is in agreement with the much lower magnetic susceptibility in the yellow-brown part (AF-2). Nghiem et al. (2020) already observed this general trend where a high abundance of ferrihydrite and goethite and a low abundance of Fe(II) minerals is characteristic for aquifer sediments low in dissolved As. The presence of magnetite in some layers (Fig. 3), where magnetic susceptibility is also high (Fig. 2), could be indicative of a transition towards a more reduced

state (Nghiem et al., 2020), which would also explain the yellow-brown rather than orange color typical for low As aquifers. The suboxic state of this part of the aquifer is also visible in the As speciation where As(V) is mainly present and represents >50% of the As pool down to a depth of 40 m and no As bearing sulfides are detectable. At 31 m depth, siderite shows its highest abundance (15% of Fe minerals) within the investigated core segments. This is in contrast to the yellow-brown color, the absence of other reduced Fe species, and the dominance of As(V). Siderite can be formed straight after the onset of reducing conditions (Kontny et al., 2021). Thus, the presence of siderite could be an early indicator for the intrusion of reducing water preferentially drawn in from the Holocene aquifer at this depth. Despite the absence of measurable CH_4 in the groundwater in this part of the aquifer, methanogens and methanotrophs represent the majority of the sedimentary microbial community (Fig. 4), suggesting a rapid consumption of CH_4 and biomass build-up, typical for a cryptic methane cycle similar to other cryptic biogeochemical cycles (Kappler and Bryce, 2017).

The situation is different below approximately 42 m, i.e., at the aquifer section located above the bottom aquitard (AT-3). Despite the fact that the groundwater is suboxic even with traces of sulfate, the Fe mineralogy (decreasing proportion of goethite, presence of green rust, Fe sulfides and carbonates) and As speciation (dominance of As(III); high abundance of As bearing sulfides) clearly points towards strongly reducing processes. At the transition to the lower aquitard (AT-3; 42.9 m), strongly reducing conditions occur, as indicated by the low abundance of goethite but the presence of siderite, a relatively high abundance of Fe sulfides and reduced As species, with arsenopyrite as major As mineral (Figs. 2 and 3). The formation of Fe and As sulfides seems to be an important immobilization mechanism for As, as shown by the high concentration of Fe_2 (6.1 wt% Fe_2O_3) and As (11 mg/kg). Overall, the entire transition zone seems to be highly reactive. Siderite, green rust and arsenopyrite are mainly present here, indicating an in-situ formation as response to the intruding reducing water.

3.2. Effect of fermentation, methanogenesis and methanotrophy on Fe redox dynamics

3.2.1. Link between fermentation and Fe cycling

The top aquitard (AT-1 and AT-2) consisting of silty clays seems to be hydraulically connected with the underlying sandy aquifers via sand lenses that are locally present (Stopelli et al., 2020). The aquitard, rich in total carbon (TC) (Fig. 2), supports the presence of various groups of microorganisms involved in C turnover, such as fermenters, methanogens and methanotrophs (Figs. 4 and 5). Among known fermenters *Chloroflexi*, *Firmicutes* and *Aminicenantales* (Gupta et al., 2014; Kampmann et al., 2012) were the most abundant taxa in the aquitard as well as in the aquifer (Fig. 4) with *Aminicenantales* being clearly more abundant in the gray reduced sediments (AF-1) compared to the yellow-brown sediments (AF-2) further below. Moreover, fermentation was predicted as the most abundant environmentally relevant pathway in the microbial community along the whole core (Fig. 5). The fermenters might play a particularly important role in the aquitard as key organic matter degraders. A variety of organic acids such as acetate, lactate, propionate or formate can be produced as a result of fermentation (Chapelle, 2000; McMahon and Chapelle, 1991). These compounds can be transported from the hydraulically connected aquitard to the aquifer, providing bioavailable OC to further fuel reductive dissolution or transformation of Fe(III) minerals and As mobilization. The transport of organic carbon via these connections could explain why the upper gray aquifer (AF-1), to which bioavailable OC can likely percolate from the carbon-rich aquitard (AT-1), is already reduced (20–30 m depth), while the lower aquifer (30–42.5 m), where the OC transport was limited, is not reduced yet. The volatile fatty acids analysis from sediment porewater collected at the same site indeed confirmed the presence of acetate, lactate and propionate at the depth between 24 and 27 m (Table S2), although at rather low concentrations (15–200 μM).

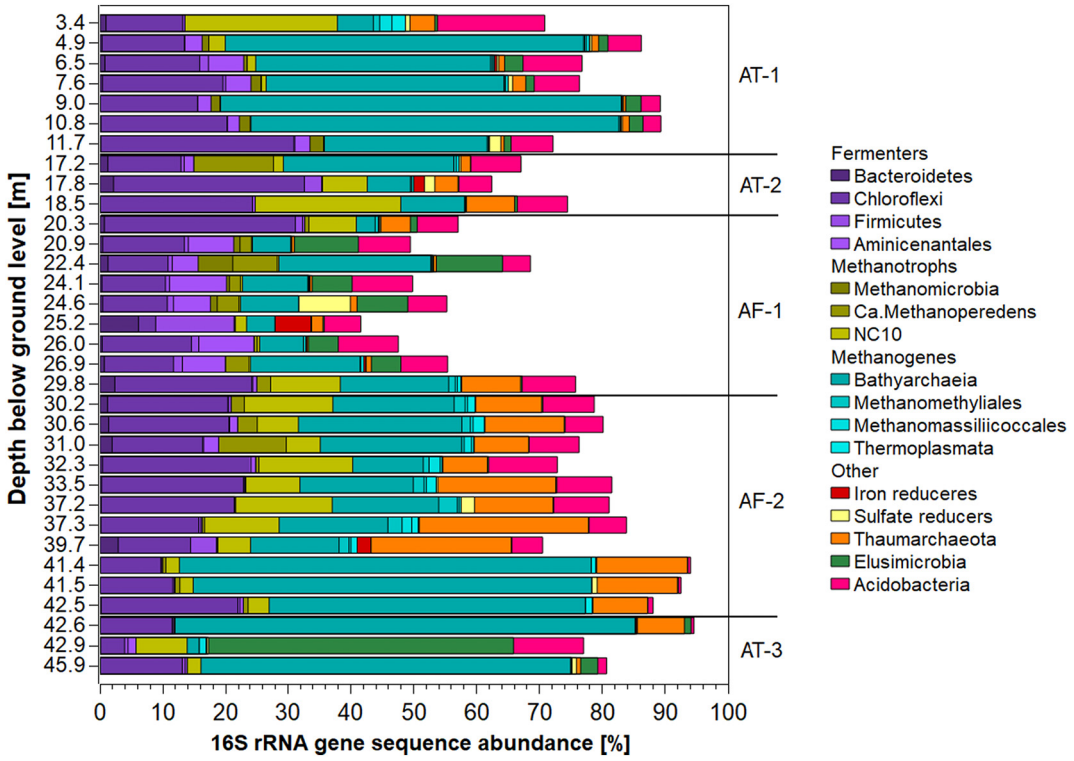

Fig. 4. Changes in relative 16S rRNA gene sequence abundance of microbial communities from samples along a redox transition zone. Taxa were grouped following their putative function in sulfate reduction, Fe(III) reduction, methanogenesis, aerobic and anaerobic methane oxidation as well as the fermentation. Top aquitard (AT-1 and AT-2), gray Holocene aquifer (AF-1), yellow-brown Pleistocene aquifer (AF-2) and bottom aquitard (AT-3).

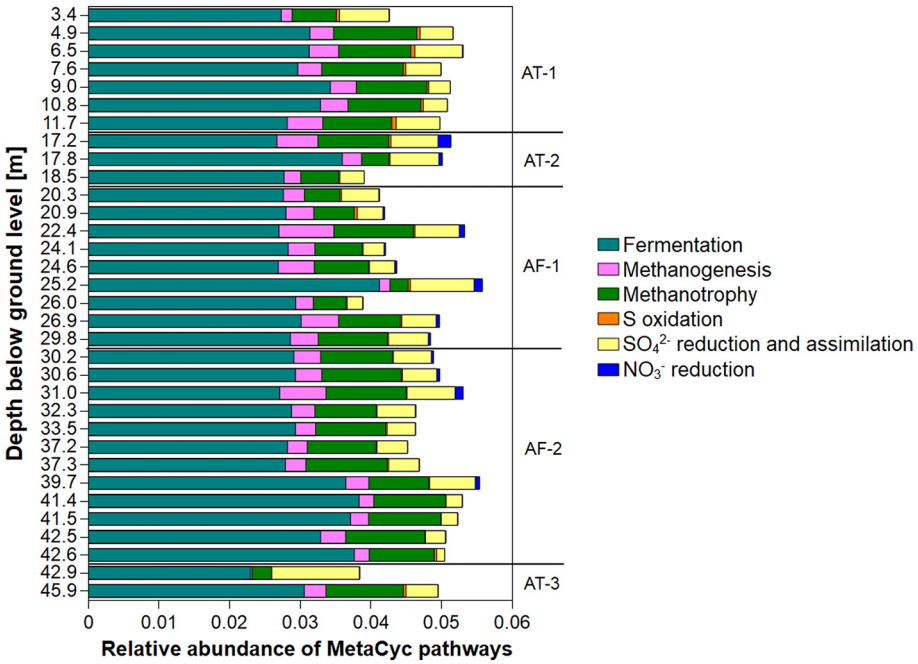

Fig. 5. Relative abundance of predicted metabolic pathways along the vertical profile of a redox transition zone. Metabolic potential was inferred from RNA-based 16S rRNA amplicon sequencing data and is based on MetaCyc pathways. Top aquitard (AT-1 and AT-2), gray Holocene aquifer (AF-1), yellow-brown Pleistocene aquifer (AF-2) and bottom aquitard (AT-3).

Although, not fully confirmed in our study, fermentation may also be directly involved in Fe and As release to groundwater. Several studies showed that significant amounts of As may be associated with natural organic matter (NOM) such as humic substances through covalent binding (Buschmann et al., 2006; Warwick et al., 2005) or via ternary metal bridging complexes with Fe and OM (Lin et al., 2004; Redman et al., 2002; Sharma et al., 2010; ThomasArrigo et al., 2014; Tipping et al., 2002). During C degradation and fermentation, these complexes may break up and release As and Fe into water. We hypothesize that the presence of binary and ternary complexes may explain generally higher As and Fe concentrations in C rich top and bottom aquitards (AT-1 and AT-22; Fig. 2) in our field site. Iron and As mobilized via fermentation could move further down the aquitard and migrate to the sandy aquifer (AF-1), overall contributing to the upper aquifer contamination, as discussed earlier (Glodowska et al., 2020c; Stopelli et al., 2020).

3.2.2. Methane production across sediment profile

Based on 16S rRNA gene sequences analysis (Fig. 4), *Bathyarchaeota* appeared to be the most abundant and omnipresent group of microorganisms across the whole vertical sediment profile, but particularly enriched in the aquitards over- (AT-1 and AT-2) and underlying (AT-3) the aquifer (64% of relative abundance at 9 m depth). Moreover, these archaea seem to be more abundant in the yellow-brown part of the aquifer (AF-2; 30–42.5 m) compared to the overlying gray part (AF-1; 20–30 m). Most members of *Bathyarchaeota* are considered as acetogens gaining energy through the reductive acetyl-CoA pathway and fermentation of various organic substrates (Feng et al., 2019; He et al., 2016). However, archaea belonging to this group were also shown to be capable of methylotrophic methanogenesis, feeding on a wide variety of methylated compounds, possessing an additional ability to ferment peptides, glucose and fatty acids (Evans et al., 2015). The identification of key genes of the MCR complex (*mcrA*, *mcrB* and *mcrG*), and the presence of *hdrABC* and *mcvhADG* responsible for the cycling of coenzyme M (CoM) and coenzyme B (CoB), further suggest their role in methanogenesis (Evans et al., 2015). This is in line with our qPCR analysis which showed that the *mcrA* gene is much more abundant in the top aquitard (AT-1 and AT-2; Fig. 6) and generally mirrors the distribution of *Bathyarchaeota* along the whole profile (Fig. 7). Therefore, it is very likely that *Bathyarchaeota* that are abundantly present at our field site are responsible for the very high CH_4 concentrations, reaching up to 51 mg/L in the AF-1 upper aquifer (Stopelli et al., 2020).

3.2.3. Methane oxidation linked to Fe and As cycling

As a consequence of the high concentrations of CH_4 in groundwater, methanotrophs also appear to be quite abundant in the sediment (Fig. 4). Among know CH_4-oxidizers, the phyla related to NC10 bacteria were the most represented, followed by a diverse group of anaerobic methane-oxidizing archaea (ANME) such as *Methanomicrobia* with dominance of *Candidatus* Methanoperedens (Fig. 4). Despite the absence of measurable CH_4 in the groundwater in the yellow-brown part of the aquifer (AF-2), methanogens and methanotrophs represent the majority of the sedimentary microbial community in this section (Fig. 4). In fact, methanotrophs and methanogens appeared to be more abundant in the lower suboxic aquifer (AF-2) compared to the upper gray, highly reduced aquifer (AF-1) where CH_4 was present at high concentration (Stopelli et al., 2020). This might suggest a rapid CH_4 turnover and justify intensive biomass build-up.

Numerous studies showed that anaerobic CH_4 oxidation can be coupled to reduction of various electron acceptors such as SO_4^{2-} (Boetius et al., 2000; Knittel and Boetius, 2009; Milucka et al., 2012; Orphan et al., 2001; Scheller et al., 2016), NO_3^- (Haroon et al., 2013), NO_2^- (Ettwig et al., 2010), Mn(IV) (Leu et al., 2020) or Fe(III) (Aromokeye et al., 2020; Cai et al., 2018; Ettwig et al., 2016). At our study site, the concentrations of NO_3^- and NO_2^- in the groundwater were below their respective detection limits; SO_4^{2-} was detected only in the deepest section of the aquifer (below 35 m) and at relatively low concentrations (max. 4.3 mg/L) (Glodowska et al., 2020c) (Table S2). Furthermore, although Mn(IV) is thermodynamically a more favorable electron acceptor than Fe(III), Mn (IV/III) was less abundant in the aquifer sediments (Fig. 2; Table S4). Therefore, Fe(III), that is ample present across the entire depth profile, seems to be the most probable electron acceptor for anaerobic CH_4 oxidation in Van Phuc.

Our previous study (Glodowska et al., 2020b) confirmed that oxidation of CH_4 was indeed coupled to Fe(III) reduction within the yellow-brown sediments, mediated by Ca. Methanoperedens, a type of archaea that was previously shown to be capable of reducing Fe(III) (Cai et al.,

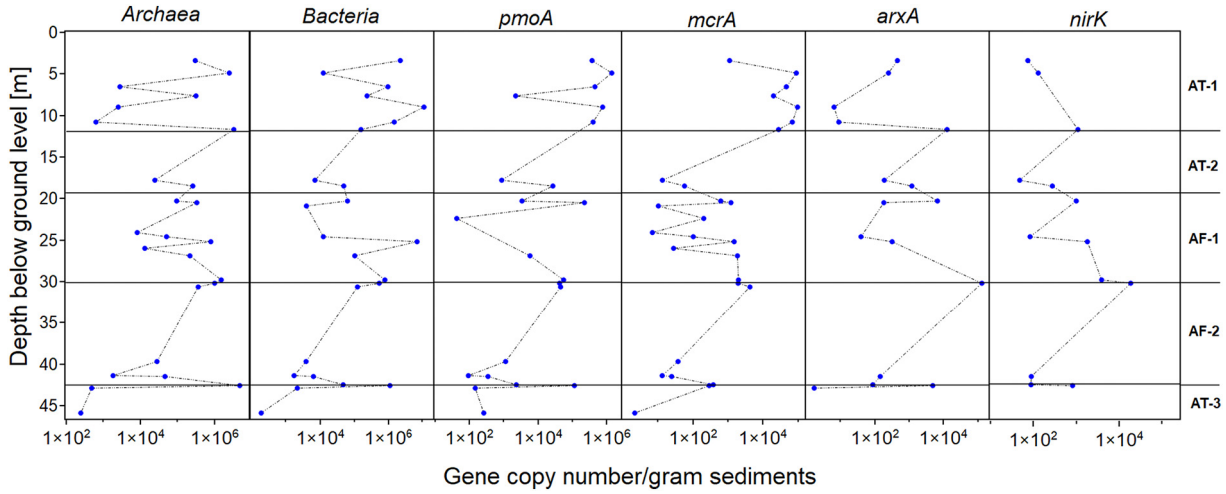

Fig. 6. Gene copy numbers (log^{10}) of archaeal and bacterial 16S rRNA genes, *pmo*A (particulate methane monooxygenase – characteristic for aerobic methane-oxidizing bacteria, also used for nitrate dependent methane oxidation) genes, *mcr*A (methyl-coenzyme M – typically used to target methanogens and anaerobic methane-oxidizing Archaea) genes, *arx*A (arsenite oxidase) genes and *nir*K (nitrite reductase) genes. Top aquitard (AT-1 and AT-2), gray Holocene aquifer (AF-1), yellow-brown Pleistocene aquifer (AF-2) and bottom aquitard (AT-3).

2018). High resolution 16S rRNA gene sequence analysis revealed that this microorganism was present across both aquifers and sporadically also in the aquitard, with particularly high abundance at 17.2 m depth (AT-2) where it represented nearly 13% of the microbial community and at 31 m (AF-2) where it accounted for 11%. This increased abundance of Ca. Methanoperedens closely coincided with two major Fe and As peaks in sediments along vertical profile (Fig. 3). At 31 m depth, the high abundance of Ca. Methanoperedens is accompanied by the maximum siderite content (15%). The relatively low Fe concentration (2.8 wt%) indicates that this Fe(III) may be reduced by Ca. Methanoperedens but instantly precipitated as siderite. The relatively high sedimentary As concentration could be related to the sorption of released As(V) to remaining goethite or its incorporation into siderite (Guo et al., 2007). Furthermore, our previous studies (Glodowska et al., 2020c, 2020b) also revealed the presence and high abundance of this archaea in some groundwater wells, particularly in those where CH_4 concentrations were elevated. A recent study by (Shi et al., 2020) showed that a similar group of ANME archaea was also involved in the reduction of As(V) in contaminated soils and sediments implying that As(V) might also be used as electron accepter. Currently, the Methanoperedens taxon is the only known Fe(III)-reducing methanotroph, but it is very likely that there are other microorganisms among the diverse group of methanotrophs found in the sediment as well as in the groundwater of Van Phuc that are able to use Fe(III) as electron acceptor and potentially affect the fate of As.

3.3. Microbially mediate Fe (trans)formation

As previously shown in batch experiments with Fe(III)-reducing bacteria, oxidizing short-chained fatty acids, ferrihydrite might be completely reduced or transformed to secondary Fe(II)-containing minerals, such as siderite (in buffered medium), magnetite or green rust (Fredrickson et al., 1998). This is in line with our observations, where sediments with a relatively low content of ferrihydrite (<10–20%) in our core are often accompanied by magnetite and partly also green rust, but not by siderite (Fig. 3). It was also shown that more crystalline Fe(III) minerals such as goethite and hematite were incubated with Fe (III)-reducing bacteria, Fe(III) was only partially reduced (Zachara et al., 2001, 1998). This could explain the residual content of hematite in the gray sediments, despite clear signs of strong reduction (Fig. 3). Based on our previous studies where we incubated orange sediments from Van Phuc either with NOM (Glodowska et al., 2020a) or CH_4 (Glodowska et al., 2020b), Fe(III) reduction mediated by *Geobacter* sp. and Ca. Methanoperedens, respectively, were accompanied by changes in sediment color from orange to dark brown/gray (Fig. S1). Most of the samples in the more suboxic part of our core have a yellow brown color indicating a partial reduction of Fe(III) minerals. Although in both cases, with NOM and with CH_4 as electron donor, some of the formed Fe(II) was released as Fe^{2+}_{aq} to groundwater, the majority of it remained in the sediments. Therefore, the incomplete reduction of Fe(III) minerals and sorption of Fe(II) onto remaining Fe(III) mineral phases likely led to the formation of Fe(II)-bearing or mixed-valence Fe minerals such as magnetite, siderite or/and green rust. Similar processes probably occur at our field site in Van Phuc as these minerals were also found at different depths across the aquifer, where the Fe(II)-bearing phases were generally more abundant in the reduced gray sediment, particularly at a depth of 26.9 m (Fig. 3). Fe(III) reduction and formation of minerals containing Fe(II) and Fe(III) cations is usually accompanied by As mobilization to the groundwater and therefore the Holocene gray sediments (AF-1) are generally associated with As-rich groundwater (Eiche et al., 2008). This is exactly what we observed in the reduced gray aquifer (AF-1) where As groundwater concentration overpassed 370 μg/L while in the deepest part of the Pleistocene aquifer (AF-2) it was below 10 μg/L (Table S3). Moreover, As(III) strongly dominates the upper Holocene aquifer sediment (AF-1). We hypothesize that a fraction of the As(III) is derived from the reduction of As(V) coupled to anaerobic CH_4 oxidation (Shi et al., 2020).

3.3.1. Methane oxidation and carbon degradation support carbonates formation

Microbially mediated CH_4 oxidation and C degradation (e.g., via fermentation) that are obviously important processes in Van Phuc, both increase the HCO_3^- anion concentration. In consequence, groundwater C-alkalinity in the redox transition zone is generally high, particularly in the upper gray sediments where it is between 9.2 and 12 mmol HCO_3^-/L (Table S3). In carbonate- and Fe^{2+}-rich environments such as the Holocene aquifer (AF-1) at our study site, carbonate green rust might form (Guilbaud et al., 2013). Green rust was identified at several depths, especially in the upper, gray aquitard (Fig. 3) with >10% at 26.7 m depth. Because of the presence of ferrous iron in the structure, green rusts possess reducing capabilities. Yet, it was shown that this is not the case for As(V), which is not reduced to As(III) in the presence of green rust (Jönsson and Sherman, 2008; Randall et al., 2001). However, the same studies also showed that As(V) remains adsorbed on the green rust as $(HAsO_4)^{2-}$ forms inner-sphere surface complexes, which was also the case for magnetite and siderite. Besides, As(III) could be oxidized by Fe(II)-activated goethite as it was previously reported (Amstaetter et al., 2010). This could explain the presence of As

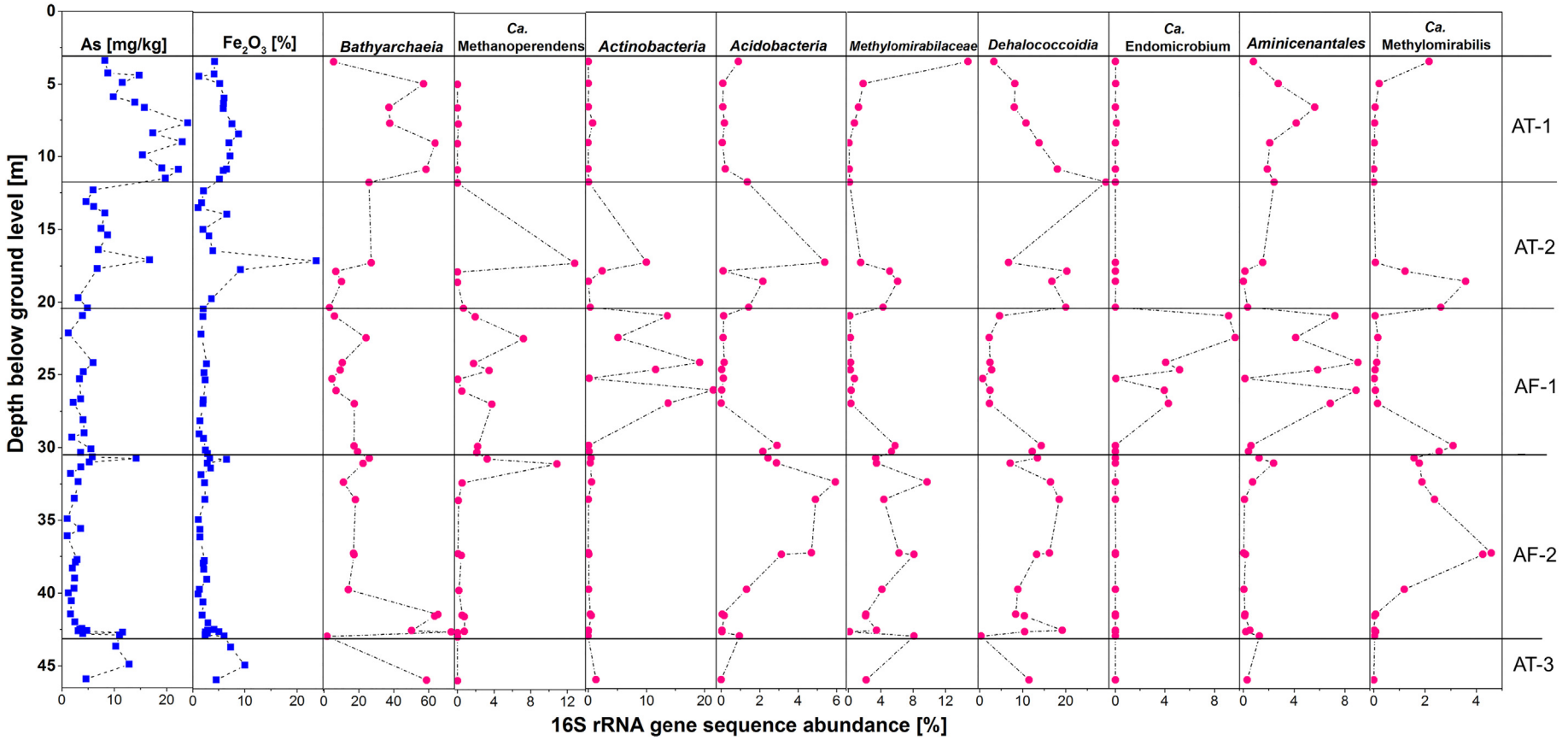

Fig. 7. Changes in relative 16S rRNA gene sequence abundance of selected taxa as well as As and Fe concentrations along the redox transition zone. Note that the x-axes are at different scales. Top aquitard (AT-1 and AT-2), gray Holocene aquifer (AF-1), yellow-brown Pleistocene aquifer (AF-2) and bottom aquitard (AT-3).

(V) accounting for up to 20% in the reduced sediments (Fig. 3). Most importantly, it was demonstrated that As(III), which is predominant in the gray part of the sediment core, also forms inner-sphere surface complexes on green rust and magnetite (Jönsson and Sherman, 2008). Therefore, green rust and magnetite, which were present across the whole profile (Fig. 3), may also play an important role as host phase for As, despite their lower abundance compared to Fe(III) (oxyhydr)oxides. In fact, the highest sedimentary As concentrations were detected at depths between 30 and 31 m which is where an increased abundance of magnetite, green rust and siderite was observed (Figs. 2 and 3).

Groundwater hydrogeochemistry can assist in understanding the mineralogical composition of the aquifer sediments. Bicarbonate likely originates from C degradation (e.g., via fermentation) and/or anaerobic CH_4 oxidation (Reeburgh, 2007; Zhu and Dittrich, 2016), but it can also result from the dissolution of carbonates already present in the sediments. Either way, HCO_3^- is the most relevant anion in the groundwater and based on saturation index calculations, the high alkalinity together with relatively high Ca concentrations (96–101 mg/L) (Stopelli et al., 2020) supports the hypothesized precipitation of carbonate minerals such as siderite or calcite. Calcite was not found in our study, however, it was detected in the aquitard of a core that was previously collected in close vicinity (Kontny et al., 2021). Therefore, Fe carbonates seem to be most relevant in this context. Uptake of As by siderite is in general less favorable than adsorption or incorporation to Fe(III) (oxyhydr)oxides (Bardelli et al., 2011). This process, however, could become environmentally relevant whenever the adsorption onto Fe(III) (oxyhydr)oxides is compromised, i.e. due to decreasing availability of sorption sites and ongoing reduction as in the gray part of the sediment (AF-1). The surface available for As sorption gradually decrease during the transformation of poorly crystalline and high-surface area minerals such as ferrihydrite towards more crystalline phases such as goethite, in addition to the change in sorption capacity and bioavailability of the more crystalline phases compared to ferrihydrite (Sracek et al., 2018). Moreover, secondary minerals such as calcite or siderite that are predicted to form at our study site (Stopelli et al., 2020) may coat the surface of highly reactive Fe(III) (oxyhydr)oxides further limiting the reductive dissolution (Vencelides et al., 2007), and at the same time reduce their sorption capacity and affinity towards As. It was recently shown that the reactivity of Fe(III) (oxyhydr)oxides such as goethite decreases in the presence of dissolved carbonate due to changes in the surface charge and aggregation (decrease of sorption sites) (Chen et al., 2020). In this scenario, carbonates, especially siderite, may play an important role is As sorption and immobilization.

The bicarbonate that is abundant in the redox transition zone might also act as a competitor for sorption sites on the Fe(III) (oxyhydr)oxides, although it has a lower affinity for adsorption than As species. The sorption affinity was shown to decrease in the following order: As(V) > PO_4^{3-} > As(III) > SiO_2 > HCO_3^- (Bang et al., 2004). It is important, however, to bear in mind that HCO_3^- is the most abundant ion present in the groundwater, typically at level of hundreds of mg/L compared to several mg/L of PO_4^{3-} or SiO_2 or to μg/L concentration of As(V) and As(III) (see Table S3), highlighting its potential importance as competitor for sorption sites. Indeed, previous laboratory studies indicated that bicarbonate ions can cause the release of As bound to sediment material (Anawar et al., 2004; Gao et al., 2013), but generally this process is believed to be rather marginal. Yet, in many aquifers (Anawar et al., 2003; García-Sánchez et al., 2005; Swartz et al., 2004), including the aquifer studied in Van Phuc (Stopelli et al., 2020), a positive correlation between dissolved As and HCO_3^- was found. This correlation, however, might rather be an effect of As release via microbially mediated reductive processes during which bicarbonate is produced as organic C or CH_4 are oxidized. Although the efficiency of HCO_3^- in replacing As from Fe(III) (oxyhydr)oxides is not fully conclusive, it appears that the presence of Ca and Mg, which are often abundant in groundwater aquifers, may enhance the As release from Fe(III) (oxyhydr)oxides (Saalfield and Bostick, 2010). The mechanism of this process, however, is not fully understood. Saalfield and Bostick (2010) pointed out that in Cambodian aquifers, which are similar to the one in Van Phuc, calcium- and bicarbonate-promoted As mobilization may take place, as As concentration tends to be highest in bicarbonate-buffered (pH 7.2–7.8), calcite-saturated waters. A predicted precipitation of dolomite in the wells with elevated As concentration (Stopelli et al., 2020) further highlights the implications of Ca, Mg and HCO_3^- for As mobility.

3.4. Abundance of unexplored putative Fe(III)-reducing microorganisms

It is well known that microorganisms can change the Fe redox state and by this indirectly affect the fate of As in groundwater. *Geobacter* (Islam et al., 2005a, 2005b, 2004) and *Shewanella* species (Cummings et al., 1999) are the most studied Fe(III)-reducers. Yet, many other microorganisms have been shown to be capable of dissimilatory Fe(III) reduction (Esther et al., 2015). Most of known Fe(III)-reducing bacteria and archaea require either organic C (e.g., short chain fatty acids, CH_4) or hydrogen (H) as electron donor (Esther et al., 2015). Interestingly, fermenters are extremely versatile organisms that can use a wide range of different organic substrates but also various electron acceptors such as Fe(III), Mn (IV), NO_3^- and NO_2^-. Representatives of the *Firmicutes* phylum, abundantly present at our field site (Fig. 4), were previously shown to use Fe(III) as electron acceptor (Esther et al., 2015). Therefore, it is possible that many fermenters present among sedimentary microbial communities across redox transition zone (Figs. 4 and 5) are in fact also involved in Fe(III) reduction and influence sediment mineralogy.

Members of the *Acidobacteria* phylum present across the entire sediment profile (Fig. 4.) are physiologically diverse and ubiquitous, especially in soils, sediment, freshwater, and polluted environments (Barns et al., 1999). *Acidobacteria* are versatile heterotrophs; therefore, it is difficult to classify them to specific functional groups. However, genomic and culture-based studies indicate the use of various carbon sources from simple sugars to more complex substrates such as hemicellulose, cellulose, and chitin (Ward et al., 2009). There is increasing evidence that *Acidobacteria* play an important role in Fe redox reactions. Not only because members of this phylum were found to be dominant in iron-rich environments (Blöthe et al., 2008; Kleinsteuber et al., 2008), but also because these bacteria seem to be genetically equipped to reduce Fe(III), although *Acidobacteria* do not use a pathway for ferric iron reduction similar to that of either *Shewanella* or *Geobacter* (Ward et al., 2009). Moreover, genome analysis revealed that members of *Acidobacteria* contained *feoAB* genes which encode a high-affinity ferrous (Fe^{2+}) iron transporter. Finally, this group of bacteria appears to be able to scavenge Fe via siderophores, although they are not equipped to biosynthesize them (Ward et al., 2009). All of these findings strongly imply that *Acidobacteria* are involved in C degradation and Fe (trans)formation but due to the lack of a pure culture this hypothesis still remains to be confirmed through future laboratory studies.

Only a few taxa such as *Geobacter* sp., *Geothrix* sp. (Islam et al., 2005b) or *Shewanella* (Cummings et al., 1999) have previously been shown to use Fe(III) as electron acceptor in As-contaminated environments. However, the microbial community present in groundwater under Fe(III)-reducing conditions (Glodowska et al., 2020c) and in sediments (Fig. 4), consists of diverse microorganisms of unexplored metabolic potential, allowing for the possibility that many of these unknown taxa can in fact also reduce Fe(III). Based on 16S rRNA gene sequencing it is quite clear that specific taxa are generally more abundant in the gray reduced sediments (AF-1), whereas others are dominating in the lower yellow-brown sediments (AF-2) (Fig. 7). *Acidobacteria* were generally more abundant at the lower part of the aquifer at the depth between 30 and 42.5 m (AF-2) and bacteria belonging to *Dehalococcoidia* were dominating in the aquitard (AT-1 and AT-2; 30% at 11.7 m), although this group was generally more abundant in the yellow-brawn sediments (AF-2) (7–19%) compared to the gray sediments (AF-1) (0.7–4.5%). On the other hand, taxa such as *Actinobacteria*, *Aminicenantales*, or Ca. Endomicrobium were clearly dominating in the gray sediments (AF-1)

(Fig. 7). There is a substantial difference between gray reduced sediments where mixed-valence Fe(II/III) minerals dominate and the groundwater is high in As versus yellow-brown sands underneath, where Fe(III) oxides prevail and groundwater has no or very little As (Eiche et al., 2008). These features create the niche for microorganisms that can not only adapt to these specific conditions but also take advantage of it. Following alpha diversity indices, the sediment in the yellow-brown suboxic aquifer (AF-2; 30–42.5 m depth) appeared to be microbially more diverse (Table S5) compared to gray reduced sediment (AF-1). Also amplicon sequencing variants (ASV) were highest in this zone, suggesting that conditions with high abundance of Fe(III) and low As concentration supports growth of more diverse microbial community, although mineralogically this zone was less diverse. Ultimately, this preferential distribution of some microorganisms across the RTZ is related to the availability of electron donors and acceptors that can support their metabolism and lifestyle.

3.5. Indication of active S-cycling

When Fe(III) reduction is taking place and sulfide is available, different Fe(II) sulfides minerals can form, including mackinawite (FeS) or pyrite (FeS_2). Iron sulfides can be found in the gray reduced part (Fig. 3), although at rather low abundance compared to other Fe minerals. One exception is at 22.2 m depth where Fe sulfides represented >20% and realgar is present. However, As (<1.5 mg/kg) and Fe_2O_3 (1.6 wt%) concentrations are particularly low at this depth. Arsenic bearing sulfides were found in the depth ranging from 21 to 28 m and again below 42 m. The presence of these minerals and detectable but rather low concentration of SO_4^{2-} in groundwater (Table S3) as well as the presence of microorganisms known to be involved in sulfate reduction (Fig. 4) and sulfur oxidation (Glodowska et al., 2020c), suggest that active S-cycling takes place in the aquifers. This is further supported by predicted SO_4^{2-} reduction and assimilation, as inferred from 16S rRNA amplicon sequences (Fig. 5). Although Fe(II) sulfides are much less abundant in the sediments compared to Fe(III) minerals, they have a very high affinity for As (Bostick et al., 2004; Bostick and Fendorf, 2003; Kirk et al., 2004). This is in line with the presence of arsenopyrite (21–28.1 m, Fig. 3) and the high As content that was found in framboidal pyrite (up to 5800 mg As/kg) at 30 m depth just a few meters away from the core position (Kontny et al., 2021). Goethite, magnetite and hematite that are often considered as the main sorbents for As are generally more abundant at the RTZ of our field site yet these minerals contain approximately 20 times less As (up to 270 μg As/g) (Kontny et al., 2021).

4. Conclusions

The high-resolution data collected in our study illustrate how challenging it is to link the activity of specific microorganisms to the mineralogical composition of the sediments and use the combined data to explain the observed As partitioning and As mobility. However, characterizing the dominant microbial groups can still be very useful to explain how specific microbial processes may affect the dynamics of Fe and As.

In our study we identified the main microbial processes in the sediments of the redox transition zone that are affecting Fe mineral (trans) formation and in consequence As dynamics. Fermentation of organic carbon seems to be a key process to increase the mobility of Fe and As in several ways. Firstly, many fermenters appear to be able to use Fe (III) as electron acceptor. Secondly, in the course of organic carbon degradation, fermenters produce more bioavailable organic compounds that can fuel the activity of Fe(III)-reducing and thus mineral-dissolving bacteria, thereby increasing As mobility. Thirdly, fermenting bacteria very likely can break binary As-OM and ternary As-Fe-OM bindings releasing both As and Fe to groundwater. Finally, fermenters together with methanotrophs increase groundwater alkalinity, and as a consequence, the biologically produced bicarbonate can either compete with As for sorption sites onto Fe(III) (oxyhydr)oxides or precipitate as carbonates, cover Fe minerals and, associated with this, reduce As sorption onto highly reactive minerals such as Fe(III) (oxyhydr)oxides. At the same time, carbonates to some extent also possess some affinity towards As, therefore potentially playing an important role in As sorption particularly when sorption sites of Fe(III)/Fe(II/III) minerals become limited. Overall, our study clearly shows that OC turnover is the main fuel leading to reductive dissolution and transformation of As-bearing Fe(III) minerals. Further studies should focus on characterizing these OC pools and on identifying the potential input of OC to the aquifer.

CRediT authorship contribution statement

Martyna Glodowska: Conceptualization, Methodology, Investigation, Writing – original draft, Writing – review & editing, Visualization. **Magnus Schneider:** Conceptualization, Methodology, Writing – review & editing, Investigation, Visualization. **Elisabeth Eiche:** Writing – original draft, Writing – review & editing, Formal analysis, Visualization. **Agnes Kontny:** Writing – review & editing, Formal analysis. **Thomas Neumann:** Supervision, Funding acquisition, Project administration. **Daniel Straub:** Data curation, Formal analysis, Software. **Michael Berg:** Supervision, Funding acquisition, Project administration, Writing – review & editing. **Henning Prommer:** Writing – review & editing, Formal analysis. **Benjamin C. Bostick:** Writing – review & editing, Methodology. **Athena A. Nghiem:** Writing – review & editing, Methodology.

Declaration of competing interest

The authors declare that they have no known competing financial interests or personal relationships that could have appeared to influence the work reported in this paper.

Acknowledgments

The authors thank all AdvectAs project members for the collaboration and support. Special thanks to Pham Hung Viet, Pham Thi Kim Trang, Vi Mai Lan, Mai Tran and Viet Nga from Hanoi University of Science for the assistance during the sampling campaign. We also thank Katja Laufer and Alyssa Findlay from Aarhus University for VFT analysis. This study was supported by the Deutsche Forschungsgemeinschaft (DFG) (KA 1736/41-1). D. Straub is funded by the Institutional Strategy of the University of Tübingen (DFG, ZUK 63) and by the Collaborative Research Center CAMPOS (Grant Agreement SFB 1253/1 2017). S. Kleindienst is funded by an Emmy-Noether fellowship (DFG, grant #326028733). The authors acknowledge support by the High Performance and Cloud Computing Group at the Zentrum für Datenverarbeitung of the University of Tübingen, the state of Baden-Württemberg through bwHPC and the German Research Foundation (DFG) through grant no INST 37/935-1 FUGG. Use of the Stanford Synchrotron Radiation Lightsource, SLAC National Accelerator Laboratory, is supported by the U.S. Department of Energy, Office of Science, Office of Basic Energy Sciences under Contract No. DE-AC02-76SF00515.

Appendix A. Supplementary data

Supplementary data to this article can be found online at https://doi.org/10.1016/j.scitotenv.2021.146501.

References

Aloisi, G., Bouloubassi, I., Heijs, S.K., Pancost, R.D., Pierre, C., Sinninghe Damsté, J.S., Gottschal, J.C., Forney, L.J., Rouchy, J.-M., 2002. CH4-consuming microorganisms and the formation of carbonate crusts at cold seeps. Earth Planet. Sci. Lett. 203, 195–203. https://doi.org/10.1016/S0012-821X(02)00878-6.

Amstaetter, K., Borch, T., Larese-Casanova, P., Kappler, A., 2010. Redox transformation of arsenic by Fe(II)-activated goethite (α-FeOOH). Environ. Sci. Technol. 44, 102–108. https://doi.org/10.1021/es901274s.

Anawar, H.M., Akai, J., Komaki, K., Terao, H., Yoshioka, T., Ishizuka, T., Safiullah, S., Kato, K., 2003. Geochemical occurrence of arsenic in groundwater of Bangladesh: sources and mobilization processes. J. Geochem. Explor. 77, 109–131. https://doi.org/10.1016/S0375-6742(02)00273-X.

Anawar, H.M., Akai, J., Sakugawa, H., 2004. Mobilization of arsenic from subsurface sediments by effect of bicarbonate ions in groundwater. Chemosphere 54, 753–762. https://doi.org/10.1016/j.chemosphere.2003.08.030.

Appelo, C.A.J., Van Der Weiden, M.J.J., Tournassat, C., Charlet, L., 2002. Surface complexation of ferrous iron and carbonate on ferrihydrite and the mobilization of arsenic. Environ. Sci. Technol. 36, 3096–3103. https://doi.org/10.1021/es010130n.

Apprill, A., McNally, S., Parsons, R., Weber, L., 2015. Minor revision to V4 region SSU rRNA 806R gene primer greatly increases detection of SAR11 bacterioplankton. Aquat. Microb. Ecol. 75, 129–137. https://doi.org/10.3354/ame01753.

Aromokeye, D.A., Kulkarni, A.C., Elvert, M., Wegener, G., Henkel, S., Coffinet, S., Eickhorst, T., Oni, O.E., Richter-Heitmann, T., Schnakenberg, A., Taubner, H., Wunder, L., Yin, X., Zhu, Q., Hinrichs, K.-U., Kasten, S., Friedrich, M.W., 2020. Rates and microbial players of iron-driven anaerobic oxidation of methane in methanic marine sediments. Front. Microbiol. 10. https://doi.org/10.3389/fmicb.2019.03041.

Bang, S., Meng, X., Bang, S., Meng, X., 2004. A review of arsenic interactions with anions and iron hydroxides. Environ. Eng. Res. 9, 184–192 (doi:2004.9.4.184).

Bardelli, F., Benvenuti, M., Costagliola, P., Di Benedetto, F., Lattanzi, P., Meneghini, C., Romanelli, M., Valenzano, L., 2011. Arsenic uptake by natural calcite: an XAS study. Geochim. Cosmochim. Acta 75, 3011–3023. https://doi.org/10.1016/j.gca.2011.03.003.

Barns, S.M., Takala, S.L., Kuske, C.R., 1999. Wide distribution and diversity of members of the bacterial kingdom Acidobacterium in the environment. Appl. Environ. Microbiol. 65, 1731–1737. https://doi.org/10.1128/AEM.65.4.1731-1737.1999.

Blöthe, M., Akob, D.M., Kostka, J.E., Göschel, K., Drake, H.L., Küsel, K., 2008. pH gradient-induced heterogeneity of Fe(III)-reducing microorganisms in coal mining-associated lake sediments. Appl. Environ. Microbiol. 74, 1019–1029. https://doi.org/10.1128/AEM.01194-07.

Boetius, A., Ravenschlag, K., Schubert, C.J., Rickert, D., Widdel, F., Gieseke, A., Amann, R., Jørgensen, B.B., Witte, U., Pfannkuche, O., 2000. A marine microbial consortium apparently mediating anaerobic oxidation of methane. Nature 407, 623. https://doi.org/10.1038/35036572.

Bolyen, E., Rideout, J.R., Dillon, M.R., Bokulich, N.A., Abnet, C., Al-Ghalith, G.A., Alexander, H., Alm, E.J., Arumugam, M., Asnicar, F., Bai, Y., Bisanz, J.E., Bittinger, K., Brejnrod, A., Brislawn, C.J., Brown, C.T., Callahan, B.J., Caraballo-Rodríguez, A.M., Chase, J., Cope, E., Silva, R.D., Dorrestein, P.C., Douglas, G.M., Durall, D.M., Duvallet, C., Edwardson, C.F., Ernst, M., Estaki, M., Fouquier, J., Gauglitz, J.M., Gibson, D.L., Gonzalez, A., Gorlick, K., Guo, J., Hillmann, B., Holmes, S., Holste, H., Huttenhower, C., Huttley, G., Janssen, S., Jarmusch, A.K., Jiang, L., Kaehler, B., Kang, K.B., Keefe, C.R., Keim, P., Kelley, S.T., Knights, D., Koester, I., Kosciolek, T., Kreps, J., Langille, M.G., Lee, J., Ley, R., Liu, Y.-X., Loftfield, E., Lozupone, C., Maher, M., Marotz, C., Martin, B.D., McDonald, D., McIver, L.J., Melnik, A.V., Metcalf, J.L., Morgan, S.C., Morton, J., Naimey, A.T., Navas-Molina, J.A., Nothias, L.F., Orchanian, S.B., Pearson, T., Peoples, S.L., Petras, D., Preuss, M.L., Pruesse, E., Rasmussen, L.B., Rivers, A., Michael, S., Robeson, I.I., Rosenthal, P., Segata, N., Shaffer, M., Shiffer, A., Sinha, R., Song, S.J., Spear, J.R., Swafford, A.D., Thompson, L.R., Torres, P.J., Trinh, P., Tripathi, A., Turnbaugh, P.J., Ul-Hasan, S., van der Hooft, J.J., Vargas, F., Vázquez-Baeza, Y., Vogtmann, E., von Hippel, M., Walters, W., Wan, Y., Wang, M., Warren, J., Weber, K.C., Williamson, C.H., Willis, A.D., Xu, Z.Z., Zaneveld, J.R., Zhang, Y., Zhu, Q., Knight, R., Caporaso, J.G., 2018. QIIME 2: Reproducible, Interactive, Scalable, and Extensible Microbiome Data Science (No. e27295v2). PeerJ Inc. https://doi.org/10.7287/peerj.preprints.27295v2.

Bostick, B.C., Fendorf, S., 2003. Arsenite sorption on troilite (FeS) and pyrite (FeS2). Geochim. Cosmochim. Acta. Advances in Oxide and Sulfide Mineral Surface Chemistry 67, 909–921. https://doi.org/10.1016/S0016-7037(02)01170-5.

Bostick, B.C., Chen, C., Fendorf, S., 2004. Arsenite retention mechanisms within estuarine sediments of Pescadero. CA. Environ. Sci. Technol. 38, 3299–3304. https://doi.org/10.1021/es035006d.

Buschmann, J., Kappeler, A., Lindauer, U., Kistler, D., Berg, M., Sigg, L., 2006. Arsenite and arsenate binding to dissolved humic acids: influence of pH, type of humic acid, and aluminum. Environ. Sci. Technol. 40, 6015–6020.

Buschmann, J., Berg, M., 2009. Impact of sulfate reduction on the scale of arsenic contamination in groundwater of the Mekong, Bengal and Red River deltas. Appl. Geochem. 24 (7), 1278–1286.

Cai, C., Leu, A.O., Xie, G.-J., Guo, J., Feng, Y., Zhao, J.-X., Tyson, G.W., Yuan, Z., Hu, S., 2018. A methanotrophic archaeon couples anaerobic oxidation of methane to Fe(III) reduction. ISME J. 12, 1929–1939. https://doi.org/10.1038/s41396-018-0109-x.

Callahan, B.J., McMurdie, P.J., Rosen, M.J., Han, A.W., Johnson, A.J.A., Holmes, S.P., 2016. DADA2: high-resolution sample inference from Illumina amplicon data. Nat. Methods 13, 581–583. https://doi.org/10.1038/nmeth.3869.

Chapelle, F.H., 2000. Ground-water Microbiology and Geochemistry. John Wiley & Sons.

Chatain, V., Bayard, R., Sanchez, F., Moszkowicz, P., Gourdon, R., 2005. Effect of indigenous bacterial activity on arsenic mobilization under anaerobic conditions. Environ. Int. Recent Advances in Bioremediation 31, 221–226. https://doi.org/10.1016/j.envint.2004.09.019.

Chen, G., Hofstetter, T.B., Gorski, C.A., 2020. Role of carbonate in thermodynamic relationships describing pollutant reduction kinetics by iron oxide-bound Fe2+. Environ. Sci. Technol. 54, 10109–10117. https://doi.org/10.1021/acs.est.0c02959.

Chowdhury, T.R., Basu, G.K., Mandal, B.K., Biswas, B.K., Samanta, G., Chowdhury, U.K., Chanda, C.R., Lodh, D., Roy, S.L., Saha, K.C., Roy, S., Kabir, S., Quamruzzaman, Q., Chakraborti, D., 1999. Arsenic poisoning in the Ganges delta. Nature 401, 545–546. https://doi.org/10.1038/44056.

Cornell, R.M., Schwertmann, U., 2003. The Iron Oxides: Structure, Properties, Reactions, Occurences and Uses. 1st ed. Wiley https://doi.org/10.1002/3527602097.

Cummings, D.E., Caccavo, Frank, Fendorf, S., Rosenzweig, R.F., 1999. Arsenic mobilization by the dissimilatory Fe(III)-reducing bacterium Shewanella alga BrY. Environ. Sci. Technol. 33, 723–729. https://doi.org/10.1021/es980541c.

Egger, M., Rasigraf, O., Sapart, C.J., Jilbert, T., Jetten, M.S.M., Röckmann, T., van der Veen, C., Bândă, N., Kartal, B., Ettwig, K.F., Slomp, C.P., 2015. Iron-mediated anaerobic oxidation of methane in brackish coastal sediments. Environ. Sci. Technol. 49, 277–283. https://doi.org/10.1021/es503663z.

Eiche, E., Neumann, T., Berg, M., Weinman, B., van Geen, A., Norra, S., Berner, Z., Trang, P.T.K., Viet, P.H., Stüben, D., 2008. Geochemical processes underlying a sharp contrast in groundwater arsenic concentrations in a village on the Red River delta, Vietnam. Appl. Geochem. Arsenic in groundwaters of South-East Asia: With emphasis on Cambodia and Vietnam 23, 3143–3154. https://doi.org/10.1016/j.apgeochem.2008.06.023.

Eiche, E., Berg, M., Hönig, S.-M., Neumann, T., Lan, V.M., Pham, T.K.T., Pham, H.V., 2017. Origin and availability of organic matter leading to arsenic mobilisation in aquifers of the Red River Delta, Vietnam. Appl. Geochem. Environmental and Health Roles of Geogenic Arsenic 77, 184–193. https://doi.org/10.1016/j.apgeochem.2016.01.006.

Esther, J., Sukla, L.B., Pradhan, N., Panda, S., 2015. Fe (III) reduction strategies of dissimilatory iron reducing bacteria. Korean J. Chem. Eng. 32, 1–14. https://doi.org/10.1007/s11814-014-0286-x.

Ettwig, K.F., Butler, M.K., Le Paslier, D., Pelletier, E., Mangenot, S., Kuypers, M.M.M., Schreiber, F., Dutilh, B.E., Zedelius, J., de Beer, D., Gloerich, J., Wessels, H.J.C.T., van Alen, T., Luesken, F., Wu, M.L., van de Pas-Schoonen, K.T., Op den Camp, H.J.M., Janssen-Megens, E.M., Francoijs, K.-J., Stunnenberg, H., Weissenbach, J., Jetten, M.S.M., Strous, M., 2010. Nitrite-driven anaerobic methane oxidation by oxygenic bacteria. Nature 464, 543–548. https://doi.org/10.1038/nature08883.

Ettwig, K.F., Zhu, B., Speth, D., Keltjens, J.T., Jetten, M.S.M., Kartal, B., 2016. Archaea catalyze iron-dependent anaerobic oxidation of methane. Proc. Natl. Acad. Sci. 113, 12792. https://doi.org/10.1073/pnas.1609534113.

Evans, P.N., Parks, D.H., Chadwick, G.L., Robbins, S.J., Orphan, V.J., Golding, S.D., Tyson, G.W., 2015. Methane metabolism in the archaeal phylum Bathyarchaeota revealed by genome-centric metagenomics. Science 350, 434–438. https://doi.org/10.1126/science.aac7745.

Ewels, P.A., Peltzer, A., Fillinger, S., Patel, H., Alneberg, J., Wilm, A., Garcia, M.U., Di Tommaso, P., Nahnsen, S., 2020. The nf-core framework for community-curated bioinformatics pipelines. Nat. Biotechnol. 38, 276–278. https://doi.org/10.1038/s41587-020-0439-x.

Feng, X., Wang, Y., Zubin, R., Wang, F., 2019. Core metabolic features and hot origin of Bathyarchaeota. Engineering 5, 498–504. https://doi.org/10.1016/j.eng.2019.01.011.

Fredrickson, J.K., Zachara, J.M., Kennedy, D.W., Dong, H., Onstott, T.C., Hinman, N.W., Li, S., 1998. Biogenic iron mineralization accompanying the dissimilatory reduction of hydrous ferric oxide by a groundwater bacterium. Geochim. Cosmochim. Acta 62, 3239–3257. https://doi.org/10.1016/S0016-7037(98)00243-9.

Gao, X., Su, C., Wang, Y., Hu, Q., 2013. Mobility of arsenic in aquifer sediments at Datong Basin, northern China: effect of bicarbonate and phosphate. J. Geochem. Explor. Arsenic, Fluoride and Iodine in Groundwater of China 135, 93–103. https://doi.org/10.1016/j.gexplo.2012.09.001.

García-Sánchez, A., Moyano, A., Mayorga, P., 2005. High arsenic contents in groundwater of central Spain. Environ. Geol. 47, 847–854. https://doi.org/10.1007/s00254-004-1216-8.

Glodowska, Stopelli, E., Schneider, M., Lightfoot, A., Rathi, B., Straub, D., Patzner, M., Duyen, V.T., Members, A.T., Berg, M., 2020a. Role of in situ natural organic matter in mobilizing as during microbial reduction of FeIII-mineral-bearing aquifer sediments from Hanoi (Vietnam). Environ. Sci. Technol. 54, 4149–4159.

Glodowska, Stopelli, E., Schneider, M., Rathi, B., Straub, D., Lightfoot, A., Kipfer, R., Berg, M., Jetten, M., Kleindienst, S., Kappler, A., 2020b. Arsenic mobilization by anaerobic iron-dependent methane oxidation. Commun. Earth Environ. 1, 1–7. https://doi.org/10.1038/s43247-020-00037-y.

Glodowska, Stopelli, E., Straub, D., Vu Thi, D., Trang, P.T.K., Viet, P.H., AdvectAs team members, Berg, M., Kappler, A., Kleindienst, S., 2020c. Arsenic behavior in groundwater in Hanoi (Vietnam) influenced by a complex biogeochemical network of iron, methane, and sulfur cycling. J. Hazard. Mater. 124398. https://doi.org/10.1016/j.jhazmat.2020.124398.

Guilbaud, R., White, M.L., Poulton, S.W., 2013. Surface charge and growth of sulphate and carbonate green rust in aqueous media. Geochim. Cosmochim. Acta 108, 141–153. https://doi.org/10.1016/j.gca.2013.01.017.

Guo, H., Stüben, D., Berner, Z., 2007. Adsorption of arsenic(III) and arsenic(V) from groundwater using natural siderite as the adsorbent. J. Colloid Interface Sci. 315, 47–53. https://doi.org/10.1016/j.jcis.2007.06.035.

Guo, H., Li, Y., Zhao, K., 2010. Arsenate removal from aqueous solution using synthetic siderite. J. Hazard. Mater. 176, 174–180. https://doi.org/10.1016/j.jhazmat.2009.11.009.

Gupta, M., Velayutham, P., Elbeshbishy, E., Hafez, H., Khafipour, E., Derakhshani, H., El Naggar, M.H., Levin, D.B., Nakhla, G., 2014. Co-fermentation of glucose, starch, and cellulose for mesophilic biohydrogen production. Int. J. Hydrog. Energy 39, 20958–20967. https://doi.org/10.1016/j.ijhydene.2014.10.079.

Haroon, M.F., Hu, S., Shi, Y., Imelfort, M., Keller, J., Hugenholtz, P., Yuan, Z., Tyson, G.W., 2013. Anaerobic oxidation of methane coupled to nitrate reduction in a novel archaeal lineage. Nature 500, 567–570. https://doi.org/10.1038/nature12375.

Harvey, C.F., Swartz, C.H., Badruzzaman, A.B.M., Keon-Blute, N., Yu, W., Ali, M.A., Jay, J., Beckie, R., Niedan, V., Brabander, D., Oates, P.M., Ashfaque, K.N., Islam, S., Hemond, H.F., Ahmed, M.F., 2002. Arsenic mobility and groundwater extraction in Bangladesh. Science 298, 1602–1606. https://doi.org/10.1126/science.1076978.

He, Y., Li, M., Perumal, V., Feng, X., Fang, J., Xie, J., Sievert, S.M., Wang, F., 2016. Genomic and enzymatic evidence for acetogenesis among multiple lineages of the archaeal

phylum Bathyarchaeota widespread in marine sediments. Nat. Microbiol. 1, 1–9. https://doi.org/10.1038/nmicrobiol.2016.35.
Horneman, A., van Geen, A., Kent, D.V., Mathe, P.E., Zheng, Y., Dhar, R.K., O'Connell, S., Hoque, M.A., Aziz, Z., Shamsudduha, M., Seddique, A.A., Ahmed, K.M., 2004. Decoupling of As and Fe release to Bangladesh groundwater under reducing conditions. Part I: evidence from sediment profiles1 1Associate editor: G. Sposito. Geochim. Cosmochim. Acta 68, 3459–3473. https://doi.org/10.1016/j.gca.2004.01.026.
Islam, F.S., Gault, A.G., Boothman, C., Polya, D.A., Charnock, J.M., Chatterjee, D., Lloyd, J.R., 2004. Role of metal-reducing bacteria in arsenic release from Bengal delta sediments. Nature 430, 68–71. https://doi.org/10.1038/nature02638.
Islam, F.S., Boothman, C., Gault, A.G., Polya, D.A., Lloyd, J.R., 2005a. Potential role of the Fe (III)-reducing bacteria Geobacter and Geothrix in controlling arsenic solubility in Bengal delta sediments. Mineral. Mag. 69, 865–875. https://doi.org/10.1180/0026461056950294.
Islam, F.S., Pederick, R.L., Gault, A.G., Adams, L.K., Polya, D.A., Charnock, J.M., Lloyd, J.R., 2005b. Interactions between the Fe(III)-reducing bacterium Geobacter sulfurreducens and arsenate, and capture of the metalloid by biogenic Fe(II). Appl. Environ. Microbiol. 71, 8642–8648. https://doi.org/10.1128/AEM.71.12.8642-8648.2005.
Jönsson, J., Sherman, D.M., 2008. Sorption of As(III) and As(V) to siderite, green rust (fougerite) and magnetite: implications for arsenic release in anoxic groundwaters. Chem. Geol. 255, 173–181. https://doi.org/10.1016/j.chemgeo.2008.06.036.
Kampmann, K., Ratering, S., Kramer, I., Schmidt, M., Zerr, W., Schnell, S., 2012. Unexpected stability of Bacteroidetes and Firmicutes communities in laboratory biogas reactors fed with different defined substrates. Appl. Environ. Microbiol. 78, 2106–2119. https://doi.org/10.1128/AEM.06394-11.
Kappler, A., Bryce, C., 2017. Cryptic biogeochemical cycles: unravelling hidden redox reactions. Environ. Microbiol. 19, 842–846. https://doi.org/10.1111/1462-2920.13687.
Keimowitz, A.R., Mailloux, B.J., Cole, P., Stute, M., Simpson, H.J., Chillrud, S.N., 2007. Laboratory investigations of enhanced sulfate reduction as a groundwater arsenic remediation strategy. Environ. Sci. Technol. 41, 6718–6724. https://doi.org/10.1021/es061957q.
King, D.W., 1998. Role of carbonate speciation on the oxidation rate of Fe(II) in aquatic systems. Environ. Sci. Technol. 32, 2997–3003. https://doi.org/10.1021/es980206o.
Kirk, M.F., Holm, T.R., Park, J., Jin, Q., Sanford, R.A., Fouke, B.W., Bethke, C.M., 2004. Bacterial sulfate reduction limits natural arsenic contamination in groundwater. Geology 32, 953–956. https://doi.org/10.1130/G20842.1.
Kleinsteuber, S., Müller, F.-D., Chatzinotas, A., Wendt-Potthoff, K., Harms, H., 2008. Diversity and in situ quantification of Acidobacteria subdivision 1 in an acidic mining lake. FEMS Microbiol. Ecol. 63, 107–117. https://doi.org/10.1111/j.1574-6941.2007.00402.x.
Knittel, K., Boetius, A., 2009. Anaerobic oxidation of methane: progress with an unknown process. Annu. Rev. Microbiol. 63, 311–334. https://doi.org/10.1146/annurev.micro.61.080706.093130.
Kontny, A., Schneider, M., Eiche, E., Stopelli, E., Glodowska, M., Rathi, B., Göttlicher, J., Byrne, J.M., Kappler, A., Berg, M., Vu Thi, D., Trang, P.T.K., Viet, P.H., Neumann, T., 2021. Iron mineral transformations and their impact on As (im)mobilization at redox interfaces in As-contaminated aquifers. Geochim. Cosmochim. Acta https://doi.org/10.1016/j.gca.2020.12.029.
Langille, M.G.I., Zaneveld, J., Caporaso, J.G., McDonald, D., Knights, D., Reyes, J.A., Clemente, J.C., Burkepile, D.E., Vega Thurber, R.L., Knight, R., Beiko, R.G., Huttenhower, C., 2013. Predictive functional profiling of microbial communities using 16S rRNA marker gene sequences. Nat. Biotechnol. 31, 814–821. https://doi.org/10.1038/nbt.2676.
Lein, A.Yu., Ivanov, M.V., Pimenov, N.V., Gulin, M.B., 2002. Geochemical peculiarities of the carbonate constructions formed during microbial oxidation of methane under anaerobic conditions. Microbiology 71, 78–90. https://doi.org/10.1023/A:1017906501726.
Leu, A.O., Cai, C., McIlroy, S.J., Southam, G., Orphan, V.J., Yuan, Z., Hu, S., Tyson, G.W., 2020. Anaerobic methane oxidation coupled to manganese reduction by members of the Methanoperedenaceae. ISME J., 1–12 https://doi.org/10.1038/s41396-020-0590-x.
Lin, H.-T., Wang, M.C., Li, G.-C., 2004. Complexation of arsenate with humic substance in water extract of compost. Chemosphere 56, 1105–1112.
Lovley, D.R., Phillips, E.J.P., Lonergan, D.J., 1991. Enzymic versus nonenzymic mechanisms for iron(III) reduction in aquatic sediments. Environ. Sci. Technol. 25, 1062–1067. https://doi.org/10.1021/es00018a007.
Lowers, H.A., Breit, G.N., Foster, A.L., Whitney, J., Yount, J., Uddin, Md.N., Muneem, Ad.A., 2007. Arsenic incorporation into authigenic pyrite, Bengal Basin sediment. Bangladesh. Geochim. Cosmochim. Acta 71, 2699–2717. https://doi.org/10.1016/j.gca.2007.03.022.
Lueders, T., Manefield, M., Friedrich, M.W., 2004. Enhanced sensitivity of DNA- and rRNA-based stable isotope probing by fractionation and quantitative analysis of isopycnic centrifugation gradients. Environ. Microbiol. 6, 73–78. https://doi.org/10.1046/j.1462-2920.2003.00536.x.
Martin, M., 2011. Cutadapt removes adapter sequences from high-throughput sequencing reads. EMBnet.journal 17, 10–12. doi:10.14806/ej.17.1.200
McMahon, P.B., Chapelle, F.H., 1991. Microbial production of organic acids in aquitard sediments and its role in aquifer geochemistry. Nature 349, 233–235. https://doi.org/10.1038/349233a0.
Milucka, J., Ferdelman, T.G., Polerecky, L., Franzke, D., Wegener, G., Schmid, M., Lieberwirth, I., Wagner, M., Widdel, F., Kuypers, M.M.M., 2012. Zero-valent sulphur is a key intermediate in marine methane oxidation. Nature 491, 541–546. https://doi.org/10.1038/nature11656.
Muehe, E.M., Kappler, A., 2014. Arsenic mobility and toxicity in South and South-east Asia – a review on biogeochemistry, health and socio-economic effects, remediation and risk predictions. Environ. Chem. 11, 483–495. https://doi.org/10.1071/EN13230.
Naujokas, Marisa F., Beth, Anderson, Habibul, Ahsan, Vasken, Aposhian H., Graziano, Joseph H., Claudia, Thompson, Suk, William A., 2013. The broad scope of health effects from chronic arsenic exposure: update on a worldwide public health problem. Environ. Health Perspect. 121, 295–302. https://doi.org/10.1289/ehp.1205875.
Neumann, R.B., Pracht, L.E., Polizzotto, M.L., Badruzzaman, A.B.M., Ali, M.A., 2014. Biodegradable organic carbon in sediments of an arsenic-contaminated aquifer in Bangladesh. Environ. Sci. Technol. Lett. 1, 221–225. https://doi.org/10.1021/ez5000644.
Newman, D.K., Beveridge, T.J., Morel, F., 1997. Precipitation of arsenic trisulfide by Desulfotomaculum auripigmentum. Appl. Environ. Microbiol. 63, 2022–2028.
Nghiem, A.A., Shen, Y., Stahl, M., Sun, J., Haque, E., DeYoung, B., Nguyen, K.N., Thi Mai, T., Trang, P.T.K., Pham, H.V., Mailloux, B., Harvey, C.F., van Geen, A., Bostick, B.C., 2020. Aquifer-scale observations of iron redox transformations in arsenic-impacted environments to predict future contamination. Environ. Sci. Technol. Lett. https://doi.org/10.1021/acs.estlett.0c00672.
Omoregie, E.O., Couture, R.-M., Cappellen, P.V., Corkhill, C.L., Charnock, J.M., Polya, D.A., Vaughan, D., Vanbroekhoven, K., Lloyd, J.R., 2013. Arsenic bioremediation by biogenic iron oxides and sulfides. Appl. Environ. Microbiol. 79, 4325–4335. https://doi.org/10.1128/AEM.00683-13.
Orphan, V.J., House, C.H., Hinrichs, K.-U., McKeegan, K.D., DeLong, E.F., 2001. Methane-consuming archaea revealed by directly coupled isotopic and phylogenetic analysis. Science 293, 484–487. https://doi.org/10.1126/science.1061338.
Parada, A.E., Needham, D.M., Fuhrman, J.A., 2016. Every base matters: assessing small subunit rRNA primers for marine microbiomes with mock communities, time series and global field samples. Environ. Microbiol. 18, 1403–1414. https://doi.org/10.1111/1462-2920.13023.
Pi, K., Wang, Y., Xie, X., Ma, T., Liu, Y., Su, C., Zhu, Y., Wang, Z., 2017. Remediation of arsenic-contaminated groundwater by in-situ stimulating biogenic precipitation of iron sulfides. Water Res. 109, 337–346. https://doi.org/10.1016/j.watres.2016.10.056.
Podgorski, J., Berg, M., 2020. Global threat of arsenic in groundwater. Science 368, 845–850. https://doi.org/10.1126/science.aba1510.
Pruesse, E., Quast, C., Knittel, K., Fuchs, B.M., Ludwig, W., Peplies, J., Glöckner, F.O., 2007. SILVA: a comprehensive online resource for quality checked and aligned ribosomal RNA sequence data compatible with ARB. Nucleic Acids Res. 35, 7188–7196. https://doi.org/10.1093/nar/gkm864.
Radu, T., Subacz, J.L., Phillippi, J.M., Barnett, M.O., 2005. Effects of dissolved carbonate on arsenic adsorption and mobility. Environ. Sci. Technol. 39, 7875–7882. https://doi.org/10.1021/es050481s.
Randall, S.R., Sherman, D.M., Ragnarsdottir, K.V., 2001. Sorption of As(V) on green rust (Fe4(II)Fe2(III)(OH)12SO4·3H2O) and lepidocrocite (γ-FeOOH): surface complexes from EXAFS spectroscopy. Geochim. Cosmochim. Acta 65, 1015–1023. https://doi.org/10.1016/S0016-7037(00)00593-7.
Ravenscroft, P., Brammer, H., Richards, K., 2011. Arsenic Pollution: A Global Synthesis. John Wiley & Sons.
Redman, A.D., Macalady, D.L., Ahmann, D., 2002. Natural organic matter affects arsenic speciation and sorption onto hematite. Environ. Sci. Technol. 36, 2889–2896.
Reeburgh, W.S., 2007. Oceanic methane biogeochemistry. Chem. Rev. 107, 486–513. https://doi.org/10.1021/cr050362v.
Reitner, J., Peckmann, J., Reimer, A., Schumann, G., Thiel, V., 2005. Methane-derived carbonate build-ups and associated microbial communities at cold seeps on the lower Crimean shelf (Black Sea). Facies 51, 66–79. https://doi.org/10.1007/s10347-005-0059-4.
Rittle, K.A., Drever, J.I., Colberg, P.J., 1995. Precipitation of arsenic during bacterial sulfate reduction. Geomicrobiol. J. 13 (1), 1–11.
Saalfield, S.L., Bostick, B.C., 2010. Synergistic effect of calcium and bicarbonate in enhancing arsenate release from ferrihydrite. Geochim. Cosmochim. Acta 74, 5171–5186. https://doi.org/10.1016/j.gca.2010.05.022.
Scheller, S., Yu, H., Chadwick, G.L., McGlynn, S.E., Orphan, V.J., 2016. Artificial electron acceptors decouple archaeal methane oxidation from sulfate reduction. Science 351, 703. https://doi.org/10.1126/science.aad7154.
Sharma, P., Ofner, J., Kappler, A., 2010. Formation of binary and ternary colloids and dissolved complexes of organic matter, Fe and As. Environ. Sci. Technol. 44, 4479–4485.
Shi, L.-D., Guo, T., Lv, P.-L., Niu, Z.-F., Zhou, Y.-J., Tang, X.-J., Zheng, P., Zhu, L.-Z., Zhu, Y.-G., Kappler, A., Zhao, H.-P., 2020. Coupled anaerobic methane oxidation and reductive arsenic mobilization in wetland soils. Nat. Geosci. 13, 799–805. https://doi.org/10.1038/s41561-020-00659-z.
Smedley, P.L., Kinniburgh, D.G., 2002. A review of the source, behaviour and distribution of arsenic in natural waters. Appl. Geochem. 17, 517–568. https://doi.org/10.1016/S0883-2927(02)00018-5.
Sø, H.U., Postma, D., Jakobsen, R., Larsen, F., 2008. Sorption and desorption of arsenate and arsenite on calcite. Geochim. Cosmochim. Acta 72, 5871–5884. https://doi.org/10.1016/j.gca.2008.09.023.
Sracek, O., Berg, M., Müller, B., 2018. Redox buffering and de-coupling of arsenic and iron in reducing aquifers across the Red River Delta, Vietnam, and conceptual model of decoupling processes. Environ. Sci. Pollut. Res. 25, 15954–15961. https://doi.org/10.1007/s11356-018-1801-0.
Stopelli, E., Duyen, V.T., Mai, T.T., Trang, P.T.K., Viet, P.H., Lightfoot, A., Kipfer, R., Schneider, M., Eiche, E., Kontny, A., Neumann, T., Glodowska, M., Patzner, M., Kappler, A., Kleindienst, S., Rathi, B., Cirpka, O., Bostick, B., Prommer, H., Winkel, L.H.E., Berg, M., 2020. Spatial and temporal evolution of groundwater arsenic contamination in the Red River delta, Vietnam: interplay of mobilisation and retardation processes. Sci. Total Environ. 717, 137143. https://doi.org/10.1016/j.scitotenv.2020.137143.
Straub, D., Blackwell, N., Fuentes, A.L., Peltzer, A., Nahnsen, S., Kleindienst, S., 2019. Interpretations of microbial community studies are biased by the selected 16S rRNA gene amplicon sequencing pipeline. bioRxiv, 2019.12.17.880468 https://doi.org/10.1101/2019.12.17.880468.
Sun, J., Mailloux, B.J., Chillrud, S.N., van Geen, A., Thompson, A., Bostick, B.C., 2018. Simultaneously quantifying ferrihydrite and goethite in natural sediments using the

method of standard additions with X-ray absorption spectroscopy. Chem. Geol. 476, 248–259. https://doi.org/10.1016/j.chemgeo.2017.11.021.
Sun, Y., Sun, J., Nghiem, A.A., Bostick, B.C., Ellis, T., Han, L., Li, Z., Liu, S., Han, S., Zhang, M., Xia, Y., Zheng, Y., 2021. Reduction of iron (hydr)oxide-bound arsenate: evidence from high depth resolution sampling of a reducing aquifer in Yinchuan Plain. China. J. Hazard. Mater. 406, 124615. https://doi.org/10.1016/j.jhazmat.2020.124615.
Swartz, C.H., Blute, N.K., Badruzzman, B., Ali, A., Brabander, D., Jay, J., Besancon, J., Islam, S., Hemond, H.F., Harvey, C.F., 2004. Mobility of arsenic in a Bangladesh aquifer: inferences from geochemical profiles, leaching data, and mineralogical characterization. Geochim. Cosmochim. Acta 68, 4539–4557. https://doi.org/10.1016/j.gca.2004.04.020.
ThomasArrigo, L.K., Mikutta, C., Byrne, J., Barmettler, K., Kappler, A., Kretzschmar, R., 2014. Iron and arsenic speciation and distribution in organic flocs from streambeds of an arsenic-enriched peatland. Environ. Sci. Technol. 48, 13218–13228. https://doi.org/10.1021/es503550g.
Tipping, E., Rey-Castro, C., Bryan, S.E., Hamilton-Taylor, J., 2002. Al (III) and Fe (III) binding by humic substances in freshwaters, and implications for trace metal speciation. Geochim. Cosmochim. Acta 66, 3211–3224.
Vencelides, Z., Sracek, O., Prommer, H., 2007. Modelling of iron cycling and its impact on the electron balance at a petroleum hydrocarbon contaminated site in Hnevice, Czech Republic. J. Contam. Hydrol. 89, 270–294. https://doi.org/10.1016/j.jconhyd.2006.09.003.
Ward, N.L., Challacombe, J.F., Janssen, P.H., Henrissat, B., Coutinho, P.M., Wu, M., Xie, G., Haft, D.H., Sait, M., Badger, J., Barabote, R.D., Bradley, B., Brettin, T.S., Brinkac, L.M., Bruce, D., Creasy, T., Daugherty, S.C., Davidsen, T.M., DeBoy, R.T., Detter, J.C., Dodson, R.J., Durkin, A.S., Ganapathy, A., Gwinn-Giglio, M., Han, C.S., Khouri, H., Kiss, H., Kothari, S.P., Madupu, R., Nelson, K.E., Nelson, W.C., Paulsen, I., Penn, K., Ren, Q., Rosovitz, M.J., Selengut, J.D., Shrivastava, S., Sullivan, S.A., Tapia, R., Thompson, L.S., Watkins, K.L., Yang, Q., Yu, C., Zafar, N., Zhou, L., Kuske, C.R., 2009. Three genomes from the phylum Acidobacteria provide insight into the lifestyles of these microorganisms in soils. Appl. Environ. Microbiol. 75, 2046–2056. https://doi.org/10.1128/AEM.02294-08.
Warwick, P., Inam, E., Evans, N., 2005. Arsenic's interaction with humic acid. Environ. Chem. 2, 119–124.
Water, S. on A. in D, Sciences, C. on L, Studies, D. on E, L., Council, N.R, 1999. Arsenic in Drinking Water. National Academies Press.
Ye, Y., Doak, T.G., 2009. A parsimony approach to biological pathway reconstruction/inference for genomes and metagenomes. PLoS Comput. Biol. 5. https://doi.org/10.1371/journal.pcbi.1000465.
Yokoyama, Y., Tanaka, K., Takahashi, Y., 2012. Differences in the immobilization of arsenite and arsenate by calcite. Geochim. Cosmochim. Acta 91, 202–219. https://doi.org/10.1016/j.gca.2012.05.022.
Zachara, J.M., Fredrickson, J.K., Li, S.-M., Kennedy, D.W., Smith, S.C., Gassman, P.L., 1998. Bacterial reduction of crystalline Fe (super 3+) oxides in single phase suspensions and subsurface materials. Am. Mineral. 83, 1426–1443. https://doi.org/10.2138/am-1998-11-1232.
Zachara, J.M., Fredrickson, J.K., Smith, S.C., Gassman, P.L., 2001. Solubilization of Fe(III) oxide-bound trace metals by a dissimilatory Fe(III) reducing bacterium. Geochim. Cosmochim. Acta 65, 75–93. https://doi.org/10.1016/S0016-7037(00)00500-7.
Zachara, J.M., Kukkadapu, R.K., Fredrickson, J.K., Gorby, Y.A., Smith, S.C., 2002. Biomineralization of poorly crystalline Fe(III) oxides by dissimilatory metal reducing bacteria (DMRB). Geomicrobiol J. 19, 179–207. https://doi.org/10.1080/01490450252864271.
Zhu, T., Dittrich, M., 2016. Carbonate precipitation through microbial activities in natural environment, and their potential in biotechnology: a review. Front. Bioeng. Biotechnol. 4. https://doi.org/10.3389/fbioe.2016.00004.
Zhu, Y.-G., Xue, X.-M., Kappler, A., Rosen, B.P., Meharg, A.A., 2017. Linking genes to microbial biogeochemical cycling: lessons from arsenic. Environ. Sci. Technol. 51, 7326–7339. https://doi.org/10.1021/acs.est.7b00689.